Composite Structures 171 (2017) 227–250

Contents lists available at ScienceDirect

Composite Structures

journal homepage: www.elsevier.com/locate/compstruct

Review

# Metamodel based high-fidelity stochastic analysis of composite laminates: A concise review with critical comparative assessment

S. Dey [a,*], T. Mukhopadhyay [b], S. Adhikari [b]

[a] Mechanical Engineering Department, National Institute of Technology Silchar, India
[b] College of Engineering, Swansea University, Swansea, United Kingdom

ARTICLE INFO

*Article history:*
Received 15 December 2016
Revised 15 January 2017
Accepted 19 January 2017
Available online 24 January 2017

*Keywords:*
Composite plate
Metamodel
Sampling techniques
Comparative study
Stochastic natural frequency

ABSTRACT

This paper presents a concise state-of-the-art review along with an exhaustive comparative investigation on surrogate models for critical comparative assessment of uncertainty in natural frequencies of composite plates on the basis of computational efficiency and accuracy. Both individual and combined variations of input parameters have been considered to account for the effect of low and high dimensional input parameter spaces in the surrogate based uncertainty quantification algorithms including the rate of convergence. Probabilistic characterization of the first three stochastic natural frequencies is carried out by using a finite element model that includes the effects of transverse shear deformation based on Mindlin's theory in conjunction with a layer-wise random variable approach. The results obtained by different metamodels have been compared with the results of traditional Monte Carlo simulation (MCS) method for high fidelity uncertainty quantification. The crucial issue regarding influence of sampling techniques on the performance of metamodel based uncertainty quantification has been addressed as an integral part of this article.



**Contents**



* Corresponding author.
*E-mail addresses:* infosudip@gmail.com (S. Dey), 800712@swansea.ac.uk, mukhopadhyay.mail@gmail.com (T. Mukhopadhyay).
*URLs:* https://sites.google.com/site/drsudipdey/ (S. Dey), http://www.tmukhopadhyay.com (T. Mukhopadhyay).

http://dx.doi.org/10.1016/j.compstruct.2017.01.061
0263-8223/

## 1. Introduction

The exhaustive utilization of computational power has favoured the development of very high-fidelity finite element models to deal with industrial problems. In spite of advances in capacity and speed of computer, the enormous computational cost of running complex, intricate scientific and engineering simulations makes it impractical to rely exclusively on simulation codes for the purpose of uncertainty quantification. Hence these high-fidelity models come with the drawback that they can be very-time consuming so that only a few runs of the model can be affordable. Thus these models are practically unusable in computationally intensive methods like traditional Monte Carlo simulation (MCS) based stochastic analysis that requires thousands of realizations to be carried out. In general, such complicated models can be considered as a system (often referred to I/O system), for which the output quantity of interest (O) is evaluated corresponding to a particular set of values for the input parameters (I). In case of analyses that require large number of model evaluation, it is a common practise to employ a computationally efficient surrogate or metamodel based approach, in which outputs are only evaluated for a limited set of algorithmically chosen input points and then an equivalent mathematical model is constructed to emulate the underlying mapping of the I/O system. The need of integrating the surrogate models and probabilistic approaches has significant demand for assessing the response characteristics of composite structures by accounting the uncertainties in the models as well as the random input parameters (e.g., geometrical parameters, fibre parameters and material properties) [1]. Application of laminated composites in various industries have witnessed tremendous growth in last few decades due to the benefit of light-weightiness without compromising its strength and stiffness requirement as shown in Fig. 1. Due to the dependency on a large number of parameters in complex production and fabrication processes of laminated composite plate, the system properties can be random in nature resulting in uncertainty in the response of the laminated composite plate. Therefore, to well define the original problems and enable a better understanding and characterization of the actual behaviour of the laminated composite structures, it is of prime importance that the inherent randomness in system parameters is incorporated in the analysis. While adopting a surrogate based approach for uncertainty quantification, an obvious question that a designer may have: which technique is superior to the other and on what basis should the various surrogate modelling techniques be selected. Some studies demonstrate the application of one metamodeling technique or the other, typically for a specific application exist; however, the present study reveals the comprehensive comparative studies of the various techniques in conjunction to composites to test the relative merits of different methods. Although the earlier studies investigated on the insights of the various approaches, the tests were restricted to a very small group of methods and test problems and in many cases only one problem due to the expense associated with testing. Moreover, when using multiple test problems, it is often difficult to make comparisons between problems when they belong to different classes of problems. In the present study, multiple factors contribute to the success of a given metamodeling technique, ranging from the stochasticity and dimensionality of the problem to the associated data sampling technique and the internal parameter settings of the various modelling techniques. Overall, the knowledge of the performance of different metamodeling techniques with respect to different modelling criteria is of utmost importance to designers while choosing an appropriate technique for a particular application. A concise literature review on application of different surrogate modelling techniques is presented in the trailing paragraphs.

A preferable strategy for the analyses requiring repetitive model evaluation is to utilize approximation models which are often referred to as metamodels ("model of the model" [2]) that effectively replace the expensive simulation model [3] in a computationally efficient manner. Metamodelling techniques have been widely used for design evaluation and optimization in many engineering applications; a comprehensive review of metamodelling applications in mechanical and aerospace systems can be found in the paper by Simpson et al. [4] and will therefore not be repeated here. For the interested reader, a review of metamodelling applications in optimization can be found in the articles by

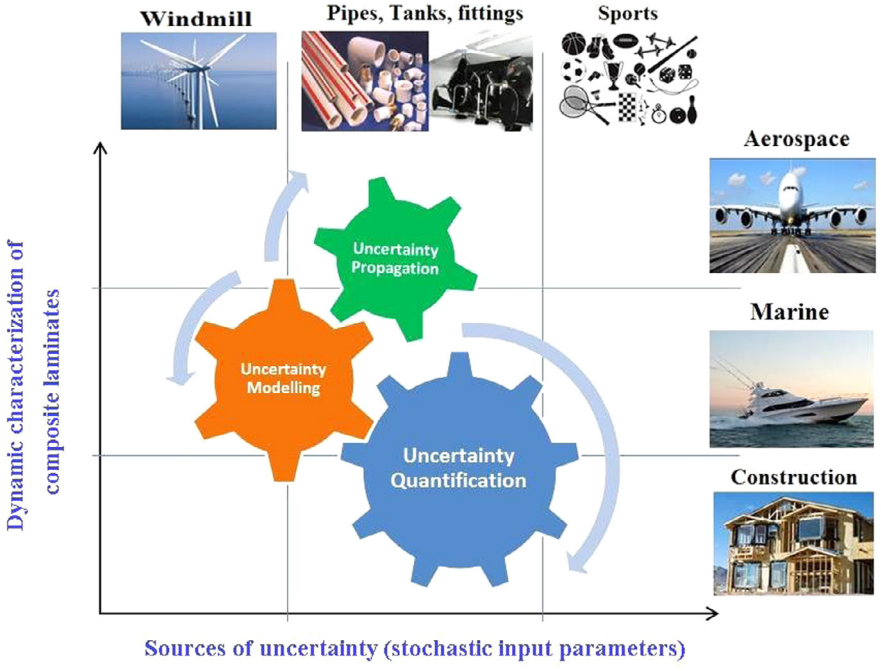


**Fig. 1.** Overview of stochastic dynamics for composite structures in different application areas.

Barthelemy and Haftka [5] and Sobieszczanski-Sobieski and Haftka [6]. A variety of surrogate modelling techniques exist wherein response surface methodology [7–9] and artificial neural network (ANN) methods [10,11] are found as the two well-known approaches for constructing simple and fast approximations of complex computer codes. An interpolation method known as Kriging is widely utilised for the design and analysis of computer experiments [12–14]. The other promising statistical techniques, such as multivariate adaptive regression splines (MARS) [15,16] and radial basis function (RBF) approximations [17,18], moving least square (MLS) [19,20], support vector regression (SVR) [21,22] and polynomial neural network (PNN) [23,24] have also drawn significant attention of many researchers. Previously, Simpson et al. [25] compared kriging methods against polynomial regression models for the multidisciplinary design optimization of an aerospike nozzle involving three design variables while Giunta et al. [26] compared kriging models and polynomial regression models for a test problem. In contrast, Varadarajan et al. [27] compared ANN methods with polynomial regression models for an engine design problem involving nonlinear thermodynamic behaviour. Yang et al. [28] compared four approximation methods such as, enhanced multivariate adaptive regression splines (MARS), stepwise regression, ANN, and the moving least square method for the construction of safety related functions in automotive crash analysis for a relatively small sample sizes.

In the literature, there are several successful applications of surrogate modelling techniques in the optimization of traditional composite laminates with straight fibers. Such as Radial Basis Functions [29], second order polynomials [30] and Neural Networks [31] are found to be effective in reducing the time to find the maximum buckling load of a composite stiffened panel. Liu et al. [32] used a cubic response surface combined with a two-level optimization technique to maximize the buckling load of a composite wing. Lee and Lin [33,34] used trigonometric functions as the base functions to build a metamodel for the stacking sequence optimization of a composite propeller. Kalnins et al. [35] compared the performance of Radial Basis Functions, multivariate adaptive regression splines and polynomials for optimization of the post-buckling characteristics of damaged composite stiffened structure. In another attempt, Lanzi and Giavotto [36] compared the performance of Radial Basis Functions, Neural Networks, and Kriging metamodels in a multi-objective optimization problem for maximum post-buckling load and minimum weight of a composite stiffened panel. These methods are found to yield similar results and none of them is identified as being significantly superior. While there is a considerable amount of existing research on the use of metamodels for constant stiffness composite design, only a few attempts look at their application in variable stiffness design. Among those worthy to mention are the following, the optimization of a variable stiffness laminate in vibration [37], the buckling load of a variable stiffness composite cylinder [38], and the simultaneous optimization of the buckling load and in-plane stiffness of a variable stiffness laminate ignoring the presence of defects, i.e. gaps and overlaps [39]. Of late, Arian Nik et al. [40,41] used the defect layer method and a Kriging metamodel to simultaneously maximize the buckling load and in-plane stiffness of a variable stiffness laminate with embedded defects. The above mentioned works are demonstrated as the potential method indicating that the surrogate model can be utilised as a beneficial tool for reduction of computational burden in optimization process. Based on literature review, it is found that in the following areas metamodeling can play a significant role: a) *Model approximation*. Approximation of computation-intensive processes across the entire design space, or global approximation, is used to reduce computation costs, b) *Design space exploration*. The design space is explored to enhance the engineers' understanding of the design problem by working on a cheap-to-run metamodel, c) *Problem formulation*. Based on an enhanced understanding of a design optimization problem, the number and search range of design variables may be reduced; certain ineffective constraints may be removed; a single objective optimization problem may be changed to a multi-objective optimization problem or vice versa. Metamodel can assist the formulation of an optimization problem that is easier to solve or more accurate than otherwise, d) *Optimization support*. Industry has various optimization needs, e.g., global optimization, multi-objective optimization, multidisciplinary design optimization, probabilistic optimization, and so on. Each type of optimization has its own challenges. Metamodeling can be applied and integrated to solve various types of optimization problems that involve computation-intensive functions. The literature review presented above reveals that there is no recommendation found regarding selection of surrogate model for analyses of composites and other applications. Furthermore, the performance of surrogate model is described as problem dependent and the best surrogate model is unknown at the outset.

For surrogate model formation, few algorithmically chosen design points are evaluated using the expensive model/ experiments. Finally on the basis of the information gathered through these design points over the design space, a fully functional metamodel is constructed. The "*Classic*" experimental designs are originated from the theory of Design of Experiments when physical experiments are conducted. These methods focus on planning experiments so that the random error in physical experiments has minimum influence in the approval or disapproval of a hypothesis. Widely used "classic" experimental designs include factorial or fractional factorial design [9,42,43], central composite design (CCD) [9], Box-Behnken [9], optimal design [44,45] and Plackett-Burman designs [9]. Mukhopadhyay et al. [46] presented a comparative assessment of different design of experiment methods in conjunction to a system identification problem using multi-objective optimization and suggested that D-optimal design and CCD perform better compared to other considered design of experiment methods. These classic methods tend to spread the sample points around boundaries of the design space and leave a few at the centre of the design space. As computer experiments involve mostly systematic error rather than random error as in physical experiments, Sacks et al. [47] stated that in the presence of systematic rather than random error, a good experimental design tends to fill the design space rather than to concentrate on the boundary. They also stated that "classic" designs, e.g. CCD and D-optimal designs can be inefficient or even inappropriate for deterministic computer codes. Jin et al. [48] confirmed that a consensus among researchers was that experimental designs for deterministic computer analyses should be space filling. Koehler and Owen [49] described several Bayesian and Frequentist "Space Filling" designs, including maximum entropy design [50], mean squared-error designs, minimax and maximin designs [51], Latin Hypercube designs, orthogonal arrays, and scrambled nets. Four types of space filling sampling methods are relatively more often used in the literature. These are orthogonal arrays [52–54], Latin Hypercube designs [55–59], Hammersley sequences [60,61] and uniform designs [62]. Hammersley sequences and uniform designs belong to a more general group called low discrepancy sequences [63] wherein Hammersley sampling is found to provide better uniformity than Latin Hypercube designs. A comparison of these sampling methods is in less structured but offer more flexibility. If any knowledge of the space is available, these methods may be tailored to achieve higher efficiency. They may also play a more active role for iterative sampling-metamodeling processes. Mainly due to the difficulty of knowing the "appropriate" sampling size a priori, sequential and adaptive sampling has gained popularity in recent years. Lin [64] proposed a sequential exploratory experiment

design (SEED) method to sequentially generate new sample points. Jin et al. [65] applied simulated annealing to quickly generate optimal sampling points. Sasena et al. [66] used the Bayesian method to adaptively identify sample points that gave more information. Wang [67] proposed an inheritable Latin Hypercube design for adaptive metamodeling. Samples are repetitively generated fitting a Kriging model in a reduced space [68]. Jin et al. [69] compared a few different sequential sampling schemes and found that sequential sampling allows engineers to control the sampling process and it is generally more efficient than one-stage sampling. One can custom design the flexible sequential sampling schemes for specific design problems.

Metamodeling evolves from classical Design of Experiments (DOE) theory, in which polynomial functions are used as response surfaces, or metamodels. Response surfaces are typically second-order polynomial models and therefore, they have limited capability to model accurately nonlinear functions of arbitrary shape. Obviously, higher-order response surfaces can be used to model a nonlinear design space. However, instabilities may arise, or it may be difficult to take enough sample points in order to estimate all of the coefficients in the polynomial equation particularly in high dimensions. Hence, many researchers advocate the use of a sequential response surface modelling approach using move limits or a trust region approach. Besides the commonly used polynomial functions, Sacks et al. [70,71] proposed the use of a stochastic model, called Kriging [72], to treat the deterministic computer response as a realization of a random function with respect to the actual system response. Neural networks have also been applied in generating the response surfaces for system approximation [73]. Other types of models include radial basis functions (RBF) [74,75], multivariate adaptive regression splines (MARS) [76], least interpolating polynomials [77] and inductive learning [78]. A combination of polynomial functions and artificial neural networks has also been archived [79]. There is no conclusion about which model is definitely superior to the others. However, insights have been gained through a number of studies [80,81]. In recent years, Kriging models and related Guassian processes are intensively studied [82–87]. In general the Kriging models are more accurate for nonlinear problems but difficult to obtain and use because a global optimization process is applied to identify the maximum likelihood estimators. Kriging is also flexible in either interpolating the sample points or filtering noisy data. On the contrary, a polynomial model is easy to construct, clear on parameter sensitivity, and cheap to work with but is less accurate than the Kriging model [48]. However, polynomial functions do not interpolate the sample points and are limited by the chosen function type. The RBF model, especially the multi-quadric RBF, can interpolate sample points and at the same time is easy to construct. It thus seems to reach a trade-off between Kriging and polynomials. Recently, a new model called Support Vector Regression (SVR) was used and tested [88]. SVR achieved high accuracy over all other metamodeling techniques including Kriging, polynomial, MARS, and RBF over a large number of test problems. It is not clear, however, what are the fundamental reasons that SVR outperformsothers. The Least Interpolating Polynomials use polynomial basis functions and also interpolate responses. They choose a polynomial basis function of "minimal degree" as described by [75] and hence are called "least interpolating polynomials." This type of metamodel deserves more study. In addition, Pérez et al. [89] transformed the matrix of second-order terms of a quadratic polynomial model into the canonical form to reduce the number of terms. Messac and his team developed an extended RBF model [90] by adding extra terms to a regular RBF model to increase its flexibility, based on which an optimal model could be searched for. Turner and Crawford proposed a NURBS-based metamodel, which was applied only to low dimensional problems [91]. If gradient information can be reliably and inexpensively obtained, gradient information can be utilized in metamodeling [92,93]. High dimensional model representation is found to be successfully applied in the problems related to optimization and system identification [93,94]. A multipoint approximation (MPA) strategy has also received some attention [95–97]. MPA uses blending functions to combine multiple local approximations, and usually gradient information is used in metamodeling. Metamodels can also be constructed when design variables are modeled as fuzzy numbers [98,99]. Each metamodel type has its associated fitting method. For example, polynomial functions are usually fitted with the (weighted) least square method; the kriging method is fitted with the search for the Best Linear Unbiased Predictor (BLUP). Simpson et al. [4] illustrated a detailed review on the equations and fitting methods for common metamodel types. In general computer experiments have very small random error which might be caused by the pseudorandom number generation or rounding [100]. Giunta et al. [101] found that numerical noises in computing the aerodynamic drag of High Speed Civil Transport (HSCT) caused many spurious local minima of the objective function. The problem was due to the discontinuous variations in calculating the drag by using the panel flow solver method. Madsen et al. [102] stated that noises could come from the complex numerical modelling techniques. In case of physical or noisy computer experiments, it is found that Kriging and RBF are more sensitive to numerical noise than polynomial models [103]. However, Kriging, RBF, and ANN could be modified to handle noises, assuming the signal to noise ratio is acceptable [104].

The different modelling methods and sampling techniques are summarized in Table 1. All of these techniques can be used to create approximations of existing computer analyses, and produce fast analysis modules for more efficient computation. These metamodeling techniques also yield insight into the functional relationship between input and output parameters. A designer's goal is usually to arrive at improved or robust solutions which are the values of design variables that best meet the design objectives. A search for these solutions usually relies on an optimization technique which generates and evaluates many potential solutions in the path toward design improvement; thus, fast analysis modules are an imperative. In the later stages of design when detailed information about specific solutions is available, highly accurate analysis is essential. In the early stages of design, however, the focus is on generating, evaluating, and comparing potential conceptual configurations. The early stages of design are characterised by a large amount of information, often uncertain, which must be managed. To ensure the identification of a 'good' system configuration, a comprehensive search is necessary. In this case, the trade-off between accuracy and efficiency may be appropriate. The creation of metamodels allows fast analysis, facilitating both comprehensive and efficient design space search at the expense of marginal loss of accuracy. Over the last few decades uncertainty quantification in complex structural systems including laminated composites has gained huge attention from the scientific community to realistically analyse and design the performance of the system [105–111]. A careful review on the literature concerning uncertainty quantification of laminated composites reveals that there are distinctively three different approaches in probabilistic modelling of such structures: random variable approach (structural and material attributes are same throughout the composite including each layers for a particular sample of Monte Carlo simulation), layer-wise random variable approach (structural and material attributes are varied layer-wise for a particular sample of Monte Carlo simulation) and random field approach (structural and material attributes are varied spatially in all the dimensions for a particular sample of Monte Carlo simulation). Recently a non-probabilistic approach of fuzzy uncertainty propagation model is proposed for

**Table 1**
Sampling techniques and metamodelling methods.

| | |
|---|---|
| 1. Sampling Techniques | a) Classic methods<br>1. Factorial Design<br>2. Central composite<br>3. Box-Behnken<br>4. Optimal designs<br>5. Plackett-Burman |
| | b) Space-filling methods<br>1. Simple Grids<br>2. Latin Hypercube<br>3. Sobol Sequence<br>4. Orthogonal Arrays (Taguchi)<br>5. Hammersley sequence<br>6. Uniform designs<br>7. Minimax and Maximin |
| | c) Hybrid methods |
| | d) Random or human selection |
| | e) Importance sampling |
| | f) Directional simulation |
| | g) Discriminative sampling |
| | h) Sequential or adaptive methods |
| 2. Modelling methods | a) Polynomial regression (linear, quadratic, or higher)<br>b) High dimensional model representation (HDMR) [cut-HDMR, RS-HDMR, GHDMR]<br>c) Polynomial Chaos Expansion (PCE)<br>d) Splines [linear, cubic, *Non-Uniform Rational B-splines* (NURBS)]<br>e) Multivariate Adaptive Regression Splines (MARS)<br>f) Gaussian Process<br>g) Kriging<br>h) Radial Basis Functions (RBF)<br>i) Least interpolating polynomials (Moving least square)<br>j) Artificial Neural Network (ANN)<br>k) Group Method of Data Handling - Polynomial Neural Network (GMDH - PNN)<br>l) Knowledge Base or Decision Tree<br>m)Support Vector Machine (SVM)<br>n) Weighted Least squares regression<br>o) Best Linear Unbiased Predictor (BLUP)<br>p) Multipoint approximation (MPA)<br>q) Sequential or adaptive metamodeling<br>r) Hybrid models |

composites that is applicable to the situation where explicit probability distribution of the material properties are not available [112]. However, uncertainty quantification based on Monte Carlo simulation based approach relies on large number of simulations. The metamodeling techniques have gained popularity to alleviate the computational burden [105–112]. A typical metamodel based algorithm for uncertainty quantification of a system is shown in Fig. 2. Performance assessment of different metamodels in uncertainty quantification of composite structures is particularly critical because of the fact that composite structures normally have a high dimensional input parameter space. Scientific literature concerning metamodeling approaches for uncertainty quantification in composite structures is not adequate. Moreover comparative assessment of different metamodeling techniques on the basis of accuracy and computational efficiency is very scarce to find in literature.

The present study investigates on stochastic structural dynamics of laminated composite plates by exhaustive utilization of surrogate modelling for uncertainty quantification. To fill up the apparent void on comparative assessment of surrogates on the basis of accuracy and computational efficiency, the this analysis

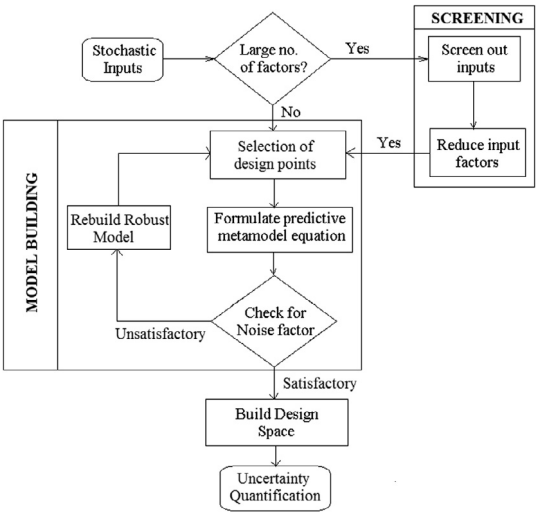


**Fig. 2.** General flowchart of Uncertainty Quantification (UQ) using metamodeling approach.

employs a finite-element model that includes the effects of transverse shear deformation based on Mindlin's theory in conjunction with a layer-wise random variable approach to study the stochastic free vibration characteristics of graphite–epoxy composite cantilever plates. An eight noded isoparametric quadratic plate bending element with five degrees of freedom at each node is considered in the finite element formulation. Both individual and combined variation of stochastic input parameters have been considered to account for the effect of dimensionality by employing the most prominent metamodeling techniques such as polynomial regression (PR), kriging, high dimensional model representation (HDMR), polynomial chaos expansion (PCE), artificial neural network (ANN), moving Least Square (MLS), support Vector Regression (SVR), multivariate adaptive regression splines (MARS), radial basis function (RBF) and polynomial neural network (PNN). For each of the surrogate modelling techniques, the rate of convergence with respect to traditional Monte Carlo simulation has been studied considering both low and high dimensional input parameter space. Different sampling techniques are used (namely $2^k$ factorial designs, central composite design, A-Optimal design, I-Optimal design, D-Optimal design, Taguchi's orthogonal array design, Box-Behnken design, Latin hypercube sampling and sobol sequence) to construct the surrogate models. The sampling technique for a particular surrogate modelling method is chosen on the basis of available literature (as furnished in Fig. 3) to ensure best possible performance of each surrogate. As an integral part of this study, a comparative assessment of different design of experiment algorithms ($2^k$ factorial designs, central composite design, A-Optimal design, I-Optimal design, D-Optimal design, Taguchi's orthogonal array design, Box-Behnken design) is presented considering polynomial regression method. To the best of authors' knowledge, this is the first attempt to investigate the comparative performance of multiple surrogates (ten most prominent models in scientific literature) in a comprehensive and exhaustive manner to provide a clear understanding of their prediction capability on the basis of accuracy and computational efficiency. This article is organized hereafter as, Section 2: finite element formulation of laminated composite plate considering layer-wise stochasticity in the input parameters, Section 3: general overview and mathematical concepts of different metamodels considered in this study, Section 4: metamodel based stochastic free vibration analysis algorithm for laminated composite plates, Section 5: results on comparative performance and discussion, Section 6: conclusion.

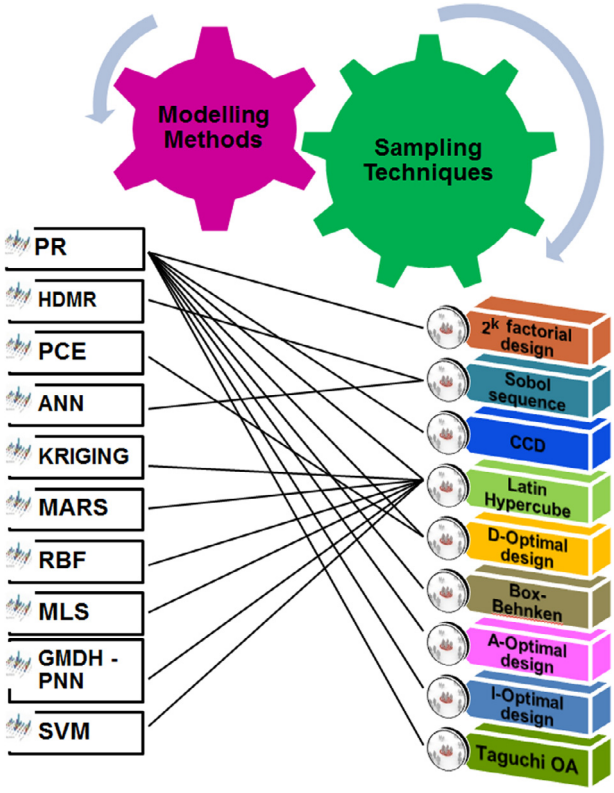


**Fig. 3.** Surrogate modelling methods and corresponding sampling techniques.

## 2. Theoretical formulation for finite element modelling of composite plate

In present study, a laminated composite cantilever plate with uniform thickness '*t*' is considered as shown in Fig. 4. Based on the first-order shear deformation theory, the displacement can be expressed as

$$\begin{aligned} u(x,y,z) &= u^0(x,y) - z\theta_x(x,y) \\ v(x,y,z) &= v^0(x,y) - z\theta_y(x,y) \\ w(x,y,z) &= w^0(x,y) = w(x,y) \end{aligned} \tag{1}$$

where, $u^0$, $v^0$, and $w^0$ are displacements of the reference plane and $\theta_x$ and $\theta_y$ are rotations of the cross section relative to x and y axes, respectively. Each of the thin fibre of laminae can be oriented at an arbitrary angle '$\theta$' with reference to the x-axis. The constitutive equations [113] are given by

$$\{F\} = [D(\bar{\omega})]\{\varepsilon\} \tag{2}$$

where Force resultant $\{F\} = \{N_x, N_y, N_{xy}, M_x, M_y, M_{xy}, Q_x, Q_y\}^T$

$$\{F\} = \left[\int_{-h/2}^{h/2} \{\sigma_x, \sigma_y, \tau_{xy}, \sigma_{xz}, \sigma_{yz}, \tau_{xyz}, \tau_{xz}, \tau_{yz}\} dz\right]^T$$

and strain $\{\varepsilon\} = \{\varepsilon_x, \varepsilon_y, \varepsilon_{xy}, k_x, k_y, k_{xy}, \gamma_{xz}, \gamma_{yz}\}^T$

The elasticity matrix of the laminated composite plate is given by,

$$[D'(\bar{\omega})] = \begin{bmatrix} A_{ij}(\bar{\omega}) & B_{ij}(\bar{\omega}) & 0 \\ B_{ij}(\bar{\omega}) & D_{ij}(\bar{\omega}) & 0 \\ 0 & 0 & S_{ij}(\bar{\omega}) \end{bmatrix} \tag{3}$$

where

$$[A_{ij}(\bar{\omega}), B_{ij}(\bar{\omega}), D_{ij}(\bar{\omega})] = \sum_{k=1}^{n} \int_{z_{k-1}}^{z_k} [\{\bar{Q}_{ij}(\bar{\omega})\}_{on}]_k [1, z, z^2] dz \quad i,j = 1,2,6$$

$$[S_{ij}(\bar{\omega})] = \sum_{k=1}^{n} \int_{z_{k-1}}^{z_k} \alpha_s [\bar{Q}_{ij}]_k dz \quad i,j = 4,5$$

where $\bar{\omega}$ indicates the stochastic representation and $\alpha$s is the shear correction factor (=5/6) and $[\bar{Q}_{ij}]$ are elements of the off-axis elastic constant matrix which is given by

$$\begin{aligned} [\bar{Q}_{ij}]_{off} &= [T_1(\bar{\omega})]^{-1} [\bar{Q}_{ij}]_{on} [T_1(\bar{\omega})]^{-T} \quad \text{for } i,j = 1,2,6 \\ [\bar{Q}_{ij}]_{off} &= [T_2(\bar{\omega})]^{-1} [\bar{Q}_{ij}]_{on} [T_2(\bar{\omega})]^{-T} \quad \text{for } i,j = 4,5 \end{aligned} \tag{4}$$

where

$$[T_1(\bar{\omega})] = \begin{bmatrix} m^2 & n^2 & 2mn \\ n^2 & m^2 & -2mn \\ -mn & mn & m^2 - n^2 \end{bmatrix} \quad \text{and} \quad [T_2(\bar{\omega})] = \begin{bmatrix} m & -n \\ n & m \end{bmatrix} \tag{5}$$

in which $m = \sin\theta(\bar{\omega})$ and $n = \cos\theta(\bar{\omega})$, wherein $\theta(\bar{\omega})$ is random ply orientation angle.

$$\begin{aligned} [Q_{ij}(\bar{\omega})]_{on} &= \begin{bmatrix} Q_{11} & Q_{12} & 0 \\ Q_{12} & Q_{12} & 0 \\ 0 & 0 & Q_{66} \end{bmatrix} \quad \text{for} \quad i,j = 1,2,6 [\bar{Q}_{ij}(\bar{\omega})]_{on} \\ &= \begin{bmatrix} Q_{44} & Q_{45} \\ Q_{45} & Q_{55} \end{bmatrix} \quad \text{for } j = 4,5 \end{aligned} \tag{6}$$

where

$$Q_{11} = \frac{E_1}{1 - nu_{12}v_{21}}, \; Q_{22} = \frac{E_2}{1 - nu_{12}v_{21}}, \; Q_{12} = \frac{v_{12}E_2}{1 - nu_{12}v_{21}}, \; Q_{66} = G_{12} \; Q_{44} = G_{23} \quad \text{and} \quad Q_{55} = G_{13}$$

An eight noded isoparametric quadratic element with five degrees of freedom at each node (three translations and two rotations) is considered in finite element formulation. The Hamilton's principle [114] is employed to study the dynamic nature of the composite structure. The principle used for the Lagrangian which is defined as

$$L_f = T - U - W \tag{7a}$$

where *T*, *U* and *W* are total kinetic energy, total strain energy and total potential of the applied load, respectively. The Hamilton's principle applicable to non-conservative system can be expressed as,

$$\delta H = \int_{t_i}^{t_f} [\delta T - \delta U - \delta W] dt = 0 \tag{7b}$$

The energy functional for Hamilton's principle is the Lagrangian ($L_f$) which includes kinetic energy ($T$) in addition to potential strain energy ($U$) of an elastic body. The expression for kinetic energy of an element is given by

$$T = \frac{1}{2}\{\dot{\delta}_e\}^T [M_e(\bar{\omega})] \tag{7c}$$

The potential strain energy for an element of a plate can be expressed as,

$$U = \frac{1}{2}\{\delta_e\}^T [K_e(\bar{\omega})]\{\delta_e\} \tag{7d}$$

The Langrange's equation of motion is given by

$$\frac{d}{dt}\left[\frac{\partial L_f}{\partial \dot{\delta}_e}\right] - \left[\frac{\partial L_f}{\partial \delta_e}\right] = \{F_e\} \tag{7e}$$

where $\{F_e\}$ is the applied external element force vector of an element and $L_f$ is the Lagrangian function. Substituting $L_f = T–U$, and the corresponding expressions for $T$ and $U$ in Lagrange's equation,

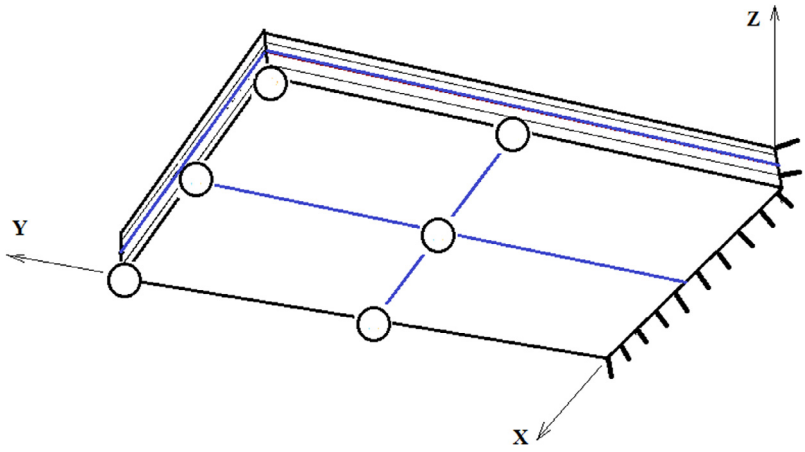


**Fig. 4.** Laminate composite cantilever plate.

one obtains the dynamic equilibrium equation for each element in the following form

$$[M(\bar{\omega})]\{\ddot{\delta}_e\} + ([K_e(\bar{\omega})])\{\delta_e\} = \{F_e\} \tag{7f}$$

After assembling all the element matrices and the force vectors with respect to the common global coordinates, the resulting equilibrium equation is obtained. For the purpose of the present study, the finite element model is developed for different element types and finite element discretization. Thus, using Hamilton's principle and Lagrange's equation, the dynamic equilibrium equation for motion of free vibration system ($\{F_e\} = 0$ i.e., without applied external element force) with $n$ degrees of freedom can be expressed as

$$[M(\bar{\omega})][\ddot{\delta}] + [K(\bar{\omega})]\{\delta\} = 0 \tag{7g}$$

In the above equation, $M(\bar{\omega}) \in R^{n\times n}$ is the mass matrix, $[K(\bar{\omega})]$ is the elastic stiffness matrix and $\{\delta\} \in R^n$is the vector of generalized coordinates. The governing equations are derived based on Mindlin's theory incorporating transverse shear deformation. For free vibration, the random natural frequencies $[\omega_n(\bar{\omega})]$ are determined from the standard eigenvalue problem [115] using QR iteration algorithm. The composite plate is assumed to be lightly damped and the natural frequencies of the system are obtained as:

$$\omega_j^2(\bar{\omega}) = \frac{1}{\lambda_j(\bar{\omega})} \quad \text{where } j = 1, 2, 3, \ldots, n_{\text{mode}} \tag{8}$$

Here $\lambda_j(\bar{\omega})$ is the $j$th stochastic eigenvalue of matrix $A = K^{-1}(\bar{\omega})M(\bar{\omega})$ and $n_{\text{mode}}$ indicates the number of modes retained in this analysis.

## 3. Mathematical formulation of metamodels

In general, the metamodels can be used as surrogates of the actual computationally expensive simulation or experimental model (refer to Fig. 5) when a large number of evaluations are needed. The metamodels thus represent the results of the structural analysis (actual model evaluation) encompassing every possible combination of all input variables. From this, thousands of combinations of all design variables can be created and performed a pseudo analysis for each variable set, by simply adopting the corresponding predictive values. The formation of metamodel is typically a three-step process. First step is selection of representative sample points (which are capable of acquiring information of the entire design space in an optimal manner), based on which the metamodel is constructed. In the second step, outputs or responses are evaluated corresponding to each sample point obtained. After obtaining the set of design points and corresponding responses, the last step is constructing the mathematical or statistical model to map input-output relationship. There exists both several sampling techniques [9,116–118] as well as metamodel formation methods [119] as discussed in Section 1. One of the main concerns is selection of appropriate DOE method and metamodelling technique for a particular problem. All the sampling methods and metamodelling techniques have their unique properties and there exists no universal model that can be regarded as the best choice for all types of problems. Sampling method and metamodelling technique for a particular problem should be chosen depending on the complexity of the model, presence of noise in sampling data, nature and dimension (number) of input parameters, desired level of accuracy and computational efficiency. Before using a particular metamodelling technique it is essential to check it rigorously for its quality of fitting and prediction capability [120–122]. Brief mathematical background of the metamodeling techniques considered in this study is presented next.

### 3.1. Polynomial regression (PR)

On the basis of statistical and mathematical analysis, the metamodelling technique gives an approximate equation which relates the input features $\xi$ and output features $y$ for aparticular system [46]

$$y = f(\xi_1, \xi_2, \ldots, \xi_k) + \epsilon \tag{9}$$

where $f$ denotes the approximate response function and $\varepsilon$ is the statistical error term having a normal distribution with mean zero and $k$ is the number of input parameters. $\xi$ is usually coded as dimensionless variable having mean zero and a standard deviation of $\xi$. The commonly used first order and second order polynomials used for this purpose are of following shapes

$$\text{First-order model (interaction)}: y = \beta_0 + \sum_{i=1}^{k}\beta_i x_i + \sum_{i=1}^{k}\sum_{j>i}^{k}\beta_{ij}x_i x_j + \varepsilon$$
$$\text{Second-order model}: y = \beta_0 + \sum_{i=1}^{k}\beta_i x_i + \sum_{i=1}^{k}\sum_{j>i}^{k}\beta_{ij}x_i x_j + \sum_{i=1}^{k}\beta_{ii}x_i^2 + \varepsilon \tag{10}$$

The metamodel is fit approximately to a set of points in the design space (which may be chosen using design of experiment approach) using a multiple regression fitting scheme.

Design of experiments (DOE) is an efficient procedure for planning experiments so that the data obtained can be utilized to

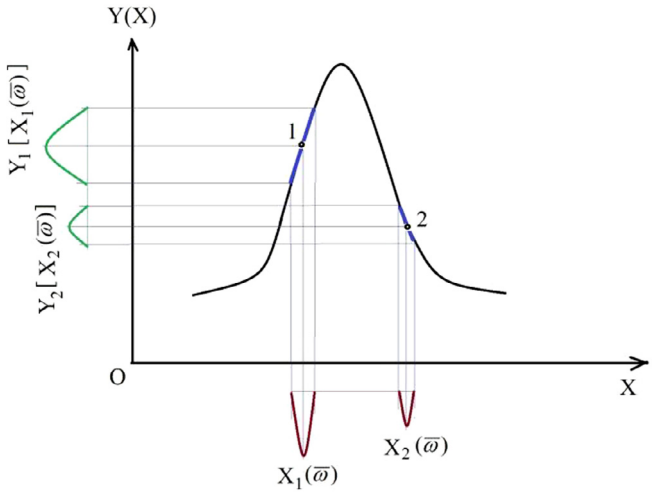


**Fig. 5.** Simulation model (Here $X$ and $Y$ represent the sets of stochastic input and output parameters, while $\bar{\omega}$ is used to denote the stochastic character). The simulation model is depicted for two different points in the design domain, indicated as 1 and 2.

achieve any particular goal. After selection of the design points using DOE, a response surface metamodel is constructed using the method of least squares. Method of least squares is a multiple regression technique and it is assumed in this method that random errors are identically distributed with a zero mean and a common unknown variance and they are independent of each other. The difference between the observed ($y$) and the fitted value ($\overline{y_i}$) for the $i$th observation $\varepsilon_i = y_i - \overline{y_i}$ is called the residual. The criterion for choosing the $\beta_i$ estimates of equation $y = X\beta + \varepsilon$ is that they should minimize the sum of the squares of the residuals, which is often called the sum of squares of the errors (*SSE*) and expressed as,

$$SSE = \sum_{i=1}^{n} \varepsilon_i^2 = \sum (y_i - \overline{y_i})^2 \tag{11}$$

The residuals may be written as

$$\varepsilon = y - X\beta \tag{12}$$

The *SSE* thus becomes

$$SSE = \varepsilon^T \varepsilon = (y - X\beta)^T (y - X\beta) \tag{13}$$

Differentiating the *SSE* with respect to $\beta$ using partial derivatives and equating it to zero, one can get $X\beta = y$. This overdetermined system of equations can be solved directly to obtain the coefficients $\beta$ as follows

$$\beta = (X^T X)^{-1} X^T y \tag{14}$$

After obtaining the coefficients $\beta$ as described above, response surface metamodel can be easily constructed. The major drawback of RSM is to fit the design points to a second order polynomial as systems having high degree of nonlinearity cannot be replaced by a second order model. To overcome this lacuna, the data can be converted into another form using suitable transformation scheme to capture the higher degree nonlinearity. For example, using logarithmic transformation or power transformation the response surface model takes the following forms,

$$\begin{aligned} \ln y &= \beta_0 + \sum_{i=1}^{k} \beta_i x_i + \sum_{i=1}^{k} \sum_{j>i}^{k} \beta_{ij} x_i x_j + \sum_{i=1}^{k} \beta_{ii} x_i^2 + \varepsilon \\ y^n &= \beta_0 + \sum_{i=1}^{k} \beta_i x_i + \sum_{i=1}^{k} \sum_{j>i}^{k} \beta_{ij} x_i x_j + \sum_{i=1}^{k} \beta_{ii} x_i^2 + \varepsilon \end{aligned} \tag{15}$$

The quality of a response surface model should be checked based on several criteria. An optimized metamodel is formed by adding or deleting input factors through backward elimination, forward addition or stepwise elimination/addition. It involves the calculation of the *P*-value (probability value, gives the risk of falsely rejecting a given hypothesis) and *Prob.* > *F* value (gives the proportion of time one would expect to get the stated *F*-value if no factor effects are significant). The metamodel constructed should be checked by some criterias such as $R^2$ (A measure of the amount of variation around the mean explained by the model), $R^2_{adj}$ (A measure of the amount of variation around the mean explained by the model, adjusted for the number of terms in the model. The adjusted R-squared decreases as the number of terms in the model increases if those additional terms don't add value to the model) and $R^2_{pred}$ (A measure of the prediction capability of the response surface model) expressed as follows.

$$R^2_{pred} = \frac{SS_R}{SS_T} = 1 - \frac{SS_E}{SS_T} \quad (0 \leqslant R^2 \leqslant 1) \tag{16}$$

$$R^2_{adj} = 1 - \frac{SS_E/(n-k-1)}{SS_T/(n-1)} = 1 - \frac{(n-1)}{(n-k-1)}(1-R^2) \quad (0 \leqslant R^2_{adj} \leqslant 1) \tag{17}$$

$$R^2_{pred} = 1 - \frac{PRESS}{SS_T} \quad (0 \leqslant R^2_{pred} \leqslant 1) \tag{18}$$

where $SS_T = SS_E + SS_R$ is the total sum of square and *PRESS* is the predicted residual error sum of squares, which is a measure of how the model fits the samples in the design space. The values of $R^2$, $R^2_{adj}$ and $R^2_{pred}$ should be close to 1. A difference between $R^2_{adj}$ and $R^2_{pred}$ within 0.2 indicates that the model can be used for further prediction. Another check is Adequate precision, which compares the range of the predicted values at the design points to the average prediction error. In general, a value greater than four indicates adequate model. Further, some plots should also be checked such as normal plot of residuals (indicates whether the residuals follow a normal distribution, in which case the points will follow a straight line), residuals vs. predicted plot (plot of the residuals versus the ascending predicted response values), actual vs. predicted plot (A graph of the actual response values versus the predicted response values for the design points used for metamodel formation. It helps to detect a value, or group of values, that are not easily predicted by the model) and Box-cox plot (helps to determine the most appropriate power transformation to be applied).

### 3.2. High dimensional model representation (HDMR)

The high dimensional model representation (HDMR) can efficiently deal with large number of input parameters. This method is important because in practical applications, the variables are often correlated, for example, the cases wherein the input variables have some relations between them. Here relation can be deterministic or stochastic. For instance, large values of certain input variables may imply large or small values of some other stochastic input variables. Such relation may be controlled by some known or unknown distributions. These correlations are implicitly contained in the collected samples in practise. The HDMR can construct a proper model for prediction of the random output (say natural frequency) in the stochastic domain. The present approach can treat both independent and correlated input variables, and includes independent input variables as a special case. The role of D-MORPH in the present form of HDMR is to ensure the component functions' orthogonality in hierarchical manner. The present technique decomposes the function $\lambda(S)$ with component functions

by input parameters, $S = (S_1, S_2, \ldots, S_{kk})$. As the input parameters are independent in nature, the component functions are specifically projected by vanishing condition. Hence, it has limitation for general formulation. In contrast, a novel numerical analysis with component functions is portrayed in the problem of present context wherein a unified framework for general HDMR dealing with both correlated and independent variables are established. For different input parameters, the output is calculated as [123]

$$\lambda(S) = \lambda_0 + \sum_{i=1}^{kk} \lambda_i(S_i) + \sum_{1 \leqslant i < j \leqslant kk} \lambda_{ij}(S_i, S_j) + \cdots + \lambda_{12\ldots kk}(S_1, S_2, S_{kk}) \tag{19}$$

$$\lambda(S) = \sum_{u \subseteq kk} \lambda_u(S_u) \tag{20}$$

where $\lambda_0$ (zeroth order component function) represents the mean value. $\lambda_i(S_i)$ and $\lambda_{ij}(S_i, \ldots, S_j)$ denote the first and second order component functions, respectively while $\lambda_{12\ldots kk}(S_1, S_2, ,S_{kk})$ indicates the residual contribution by input parameters. The subset $u \subseteq \{1, 2, \ldots, kk\}$ denotes the subset where $u \subseteq kk$ for simplicity and empty set, $\Gamma \in u$. As per Hooker's definition, the correlated variables are expressed as,

$$\{\lambda_u(S_u | u \subseteq kk)\} = Arg \min_{\{g_u \in L^2(R^u), u \subseteq kk\}} \int \left( \sum_{u \subseteq k} g_u(S_u) - \lambda(S) \right)^2 w(S) dS \tag{21}$$

$$\forall u \subseteq kk, \quad \forall i \in u, \quad \int \lambda_u(S_u)\ w(S) dS_i\ dS_{-u} = 0 \tag{22}$$

$$\forall v \subset u, \quad \forall g_v : \int \lambda_u(S_u) g_v(S_v) w(S) dS = \langle \lambda_u(S_u) g_v(S_v) \rangle = 0 \tag{23}$$

The function $\lambda(S)$ can be obtained from sample data by experiments or by modelling. To minimize the computational cost, the reduction of the squared error can be realised easily. Assuming $H$ in Hilbert space is expanded on the basis $\{h_1, h_2, \ldots, h_{kk}\}$, the bigger subspace $\bar{H}$ ($\supset H$) is expanded by extended basis $\{h_1, h_2, \ldots, h_{kk}, h_{kk+1}, \ldots, h_m\}$. Then $\bar{H}$ can be decomposed as

$$\bar{H} = H \oplus H^{\perp} \tag{24}$$

where $H^{\perp}$ denotes the complement subspace (orthogonal) of $H$ [124] within $\bar{H}$. In the past work [125–127], the component functions are calculated from basis functions. The component functions of Second order HDMR expansion are estimated from basis functions $\{\varphi\}$ as [128]

$$\lambda_i(S_i) \approx \sum_{r=1}^{kk} \alpha_r^{(0)i} \varphi_r^i(S_i) \tag{25}$$

$$\lambda_{ij}(S_i, S_j) \approx \sum_{r=1}^{kk} [\alpha_r^{(ij)i} \varphi_r^i(S_i) + \alpha_r^{(ij)j} \varphi_r^j(S_j)] + \sum_{p=1}^{l} \sum_{q=1}^{l} \beta_{pq}^{(0)ij} \varphi_p^i(S_i) \varphi_q^j(S_j) \tag{26}$$

i.e., the basis functions of $\lambda_{ij}(S_i, S_j)$ contain all the basis functions used in $\lambda_i(S_i)$ and $\lambda_j(S_j)$.

The HDMR expansions at $N_{samp}$ sample points of $S$ can be represented as a linear algebraic equation system

$$\Gamma J = \hat{R} \tag{27}$$

where $\Gamma$ denotes a matrix ($N_{samp} \times \tilde{t}$) whose elements are basis functions at the $N_{samp}$ values of $S$; $J$ is a vector with $\tilde{t}$ dimension of all unknown combination coefficients; $\hat{R}$ is a vector with $N_{samp}$-dimension wherein $l$th element is $\lambda(S^{(l)}) - \lambda_0$. $S^{(l)}$ denotes the $l$th sample of $S$, and $\lambda_0$ represents the average value of all $\lambda(S^{(l)})$. The regression equation for least squares of the above equation can be expressed as

$$\frac{1}{N_{samp}} \Gamma^T \Gamma J = \frac{1}{N_{samp}} \Gamma^T \hat{R} \tag{28}$$

Due to the use of extended bases, some rows of the above equation are identical and can be removed to give an underdetermined algebraic equation system

$$AJ = \hat{V} \tag{29}$$

It has many of solutions for $J$ composing a manifold $Y \in Re^{\tilde{t}}$. Now the task is to find a solution $J$ from $Y$ to force the HDMR component functions satisfying the hierarchical orthogonal condition. D-MORPH regression provides a solution to ensure additional condition of exploration path represented by differential equation

$$\frac{dJ(l)}{dl} = \chi v(l) = (I_t - A^{+}A)\, v(l) \tag{30}$$

wherein $\chi$ denotes orthogonal projector ensuring

$$\chi^2 = \chi \quad \text{and} \quad \chi^T = \chi \tag{31}$$

$$\chi = \chi^2 = \chi^T \chi \tag{32}$$

The free function vector may be selected to ensure the wide domain for $J(l)$ as well as to simultaneously reduce the cost $\kappa(J(l))$ which can be expressed as

$$v(l) = -\frac{\partial \kappa(J(l))}{\partial J} \tag{33}$$

Then we obtain

$$\begin{aligned} \frac{\partial \kappa(J(l))}{\partial l} &= \left( \frac{\partial \kappa(J(l))}{\partial J} \right)^T \frac{\partial J(l)}{\partial l} = \left( \frac{\partial \kappa(J(l))}{\partial J} \right)^T P v(l) \\ &= -\left( P \frac{\partial \kappa(J(l))}{\partial J} \right)^T \left( P \frac{\partial \kappa(J(l))}{\partial J} \right) \leqslant 0 \end{aligned} \tag{34}$$

The cost function can be expressed in quadratic form as

$$\kappa = \frac{1}{2} J^T B J \tag{35}$$

where $B$ denotes the positive definite symmetric matrix and $J_\infty$ can be expressed as

$$J_\infty = V_t (U_{\tilde{t}-r}^T V_{\tilde{t}-r})^{-1} U_{\tilde{t}-r}^T A^{+} \hat{V} \tag{36}$$

where the last columns $(\tilde{t} - r)$ of $U$ and $V$ are denoted as $U_{\tilde{t}-r}$ and $V_{\tilde{t}-r}$ which can found by decomposition of $\chi B$ [129]

$$\chi B = U \begin{bmatrix} \bar{S}_r & 0 \\ 0 & 0 \end{bmatrix} V^T \tag{37}$$

This unique solution $J_\infty$ in $Y$ indicates the minimized cost function. D-MORPH regression is used to find the $J$ which ensures the HDMR component functions' orthogonality in hierarchical manner. The construction of the corresponding cost function $\kappa$ can be found in previous literature [125].

### 3.3. Polynomial chaos expansion (PCE)

The polynomial chaos expansion is an effective tool for solving stochastic systems. It was first introduced as the homogeneous chaos by Wiener [130]. The basic idea is to project the random variables of problem onto a stochastic space spanned by a set of

complete orthogonal polynomials. The orthogonal polynomial chaos basis functions, derived from Gram-Schmidt algorithm [131] is employed in this study for mapping input-output relation. The solution to generalized equation at a random space can be expanded into a polynomial chaos expansion as follows:

$$\mathbf{y} = \mathbf{B}\boldsymbol{\psi}(\xi) \tag{38}$$

where $\mathbf{y} = [y_1 y_2 \ldots, y_n]^T \in \Re^{n\times 1}$ denotes the assembled vector of output data, $\boldsymbol{\psi}(\xi) = [psi_0(\xi)\psi_1(\xi)\ldots\psi_p(\xi)]^T \in \Re^{p\times 1}$ denotes the assembled vector of polynomial chaos basis functions and $\mathbf{B}$ is expressed as

$$\mathbf{B} = \begin{bmatrix} \beta_0^{(1)} & \beta_1^{(1)} & \beta_2^{(1)} & \cdots & \beta_p^{(1)} \\ \beta_0^{(2)} & \beta_1^{(2)} & \beta_2^{(2)} & \cdots & \beta_p^{(2)} \\ \beta_0^{(3)} & \beta_1^{(3)} & \beta_2^{(3)} & \cdots & \beta_p^{(3)} \\ . & . & . & & . \\ . & . & . & & . \\ . & . & . & & . \\ \beta_0^{(n)} & \beta_1^{(n)} & \beta_2^{(n)} & \cdots & \beta_p^{(n)} \end{bmatrix} \tag{39}$$

where $\beta_k^{(i)}$ are the coefficients of polynomial expansion with $k$ = 1,2,3…$p$ ($p$ is the number of terms retained in the expansion), $n$ is the number of output parameters, $\xi$ is an $m$-dimensional vector of variables and '$m$' is the number of input parameters. Gram-Schmidt algorithm provides the opportunity to derive the polynomial chaos basis functions for any arbitrary probability distribution on '$\boldsymbol{\xi}$'. In this method, the polynomial terms are represented as $\psi_j(\xi_i) = \xi_i^j + O(\xi_i^{j-1})$ where $j = 0, 1, \ldots, h$. This results in $\psi_0(\xi_i) = 1$and the remaining terms are computed using the following recursive equations:

$$\psi_j(\xi_i) = e_j(\xi_i) - \sum_{k=0}^{j-1} c_{jk}\psi_k(\xi_i) \tag{40}$$

where $c_{jk} = \dfrac{\int_{\text{supp }\xi_i} e_j(\xi_i)\psi_k(\xi_i)p(\xi_i)d\xi_i}{\int_{\text{supp }\xi_i} \psi_k^2(\xi_i)p(\xi_i)p(\xi_i)d\xi_i}$

The lower and upper bounds of input variables (i.e., $p_i^{(L)}, p_i^{(U)}$) can be transformed into the normalized values of -1 and 1, respectively and thus a transformation function $\varphi(\bullet)$ for any intermediate value in the design domain can be obtained as:

$$\xi_i = \varphi(p_i) = 2\left(\frac{p_i - p_i^{(L)}}{p_i^{(U)} - p_i^{(L)}} - \frac{1}{2}\right) \tag{41}$$

$$p_i = \varphi^{-1}(\xi_i) = \frac{\left(p_i^{(U)} - p_i^{(L)}\right)}{2}\xi_i + \frac{\left(p_i^{(U)} + p_i^{(L)}\right)}{2} \tag{42}$$

where $\xi_i$ is the transformed value in domain [-1, 1] corresponding to $p_i$ in the domain $[p_i^{(L)}, p_i^{(U)}]$ for $i$th input parameter ($\boldsymbol{\xi} = [\xi_1, \xi_2, \ldots, \xi_m]^T \in \Re^{m\times 1}$).

### 3.4. Kriging method

The Kriging model initially developed in spatial statistics by Danie Gerhardus Krige and subsequently extended by Matheron [132] and Cressie [133]. Kriging is a Gaussian process based modelling method, which is compact and cost effective for computation. Kriging surrogate models are employed to fit the data those are obtained for larger experimental areas than the areas used in low order polynomial regression. Hence Kriging models are global rather than local wherein such models are used for prediction. The Kriging model postulates a combination of a known function employed for simulation of required output as

$$y(x) = y_0(x) + Z(x) \tag{43}$$

where $y(x)$ is the unknown function of interest, $x$ is an $m$ dimensional vector ($m$ design variables), $y_0(x)$ is the known approximation (usually polynomial) function and $Z(x)$ represents is the realization of a stochastic process with mean zero, variance, and nonzero covariance. In the model, the local deviation at an unknown point ($\mathbf{x}$) is expressed using stochastic processes. The sample points are interpolated with the Gaussian random function as the correlation function to estimate the trend of the stochastic processes. The $y_0(x)$ term is similar to a polynomial response surface, providing global model of the design space. In present study, $y_0(x)$ globally approximates the design space, $Z$(x) creates the localized deviations so that the Kriging model interpolative Kriging models can also be created to smooth noisy data [134]. The covariance matrix of $Z(x)$ is given as

$$Cov[Z(x^i), Z(x^j)] = \sigma^2 R[R(x^i, x^j)] \tag{44}$$

where $\boldsymbol{R}$ is a ($p \times p$) correlation matrix and $R(\boldsymbol{x}^i, \boldsymbol{x}^j)$ is the correlation function between any two of the $p$-sampled data points $\boldsymbol{x}^i$ and $\boldsymbol{x}^j$. $\boldsymbol{R}$ is an ($p \times p$) symmetric matrix with ones along the diagonal. The correlation function $R(\boldsymbol{x}^i, \boldsymbol{x}^j)$ is specified by the user, and a variety of correlation functions exist. Using Gaussian correlation function

$$R(x^i, x^j) = \exp\left[-\sum_{k=1}^{n}\theta_k\left|x_k^i - x_k^j\right|^2\right] \tag{45}$$

where $n$ is the number of design variables, $\theta_k$ is the unknown correlation parameters used to fit the model, and $x_k^i$ and $x_k^j$ are the $k$th components of the sample points $x^i$ and $x^j$, respectively. The predicted estimates, $\hat{y}$ of the response $y(x)$ at random values of $x$ are defined as Kriging predictor

$$\hat{y}(x) = \hat{\beta} + r^T(x)R^{-1}[y - f\hat{\beta}] \tag{46}$$

where $y$ is the column vector of length $p$ that contains the sample values of the frequency responses and $f$ is a column vector of length $p$ that is filled with ones when $y_0(x)$ is taken as constant. Now, $r^T(x)$ is the correlation vector of length $p$ between the random $x$ and the sample data points $\{x^1, x^2, \ldots x^p\}$

$$r^T(x) = [R(x, x^1), R(x, x^2), R(x, x^3)\ldots R(x, x^p)]^T \tag{47}$$

$$\hat{\beta} = (f^T R^{-1} f)^{-1} f^T R^{-1} y \tag{48}$$

An estimate of the variance between underlying global model $\hat{\beta}$ and $y$ is estimated by

$$\hat{\sigma}^2 = \frac{1}{p}(y - f\hat{\beta})^T R^{-1}(y - f\hat{\beta}) \tag{49}$$

Now the model fitting is accomplished by maximum likelihood (i.e., best guesses) for $\theta_k$. The maximum likelihood estimates (i.e., "best guesses") for the $\theta_k$ in Eq. (38) used to fit a Kriging model are obtained as

$$Max.\Gamma(\theta_k) = -\frac{1}{2}\left[p\ln(\hat{\sigma}^2) + ln|R|\right] \tag{50}$$

where the variance $\sigma^2$ and $|\boldsymbol{R}|$ are both functions of $\theta_k$, is solved for positive values of $\theta_k$ as optimization variables. After obtaining Kriging based surrogate, the random process $Z(\boldsymbol{x})$ provides the approximation error that can be used for improving the surrogate model. The maximum mean square error (MMSE) and maximum error (ME) are calculated as,

$$MMSE = \max.\left[\frac{1}{k}\sum_{i=1}^{k}(\bar{y}_i - y_i)^2\right] \tag{51}$$

$$ME\ (\%) = Max\left[\frac{y_{i,MCS} - y_{i,Kriging}}{Y_{i,MCS}}\right] \tag{52}$$

where $y_i$ and $\bar{y}_i$ are the vector of the true values and the vector corresponding to $i$th prediction, respectively.

### 3.5. Multivariate adaptive regression splines (MARS)

Multivariate adaptive regression splines algorithm (MARS) [135] provides an efficient mathematical relationship between input parameters and output feature of interest for a system under investigation based on few algorithmically chosen samples. MARS is a nonparametric regression procedure that makes no assumption about the underlying functional relationship between the dependent and independent variables. MARS algorithm adaptively selects a set of basis functions for approximating the response function through a forward and backward iterative approach. The MARS model can be expressed as

$$Y = \sum_{k=1}^{n} \alpha_k H_k^f(x_i) \tag{53}$$

with $H_k^f(x_1, x_2, x_3 \ldots x_n) = 1$ for $k = 1$

where $\alpha_k$ and $H_k^f(x_i)$ are the coefficient of the expansion and the basis functions, respectively. Thus the first term of Eq. (53) becomes $\alpha_1$, which is basically an intercept parameter. The basis function can be represented as

$$H_k^f(x_i) = \Pi_{i=1}^{i_k} \left[ Z_{i,k}(x_{j(i,k)} - t_{i,k}) \right]_{tr}^{q} \tag{54}$$

where $i_k$ is the number of factors (interaction order) in the $k$th basis function, $z_{i,k} = \pm 1$, $x_{j(i,k)}$ is the $j$th variable, $1 \le j(i,k) \le$ n, and $t_{i,k}$ is a knot location on each of the corresponding variables. $q$ is the order of splines. The approximation function $Y$ is composed of basis functions associated with $k$ sub-regions. Each multivariate spline basis function $H_k^f(x_i)$ is the product of univariate spline basis functions $z_{i,k}$, which is either order one or cubic, depending on the degree of continuity of the approximation. The notation "$tr$" means the function is a truncated power function.

$$\left[ z_{i,k}(x_{j(i,k)} - t_{i,k}) \right]_{tr}^{q} = \left[ z_{i,k}(x_{j(i,k)} - t_{i,k}) \right]^{q} \quad \text{for} \quad \left[ z_{i,k}(x_{j(i,k)} - t_{i,k}) \right] < 0 \tag{55}$$

$$\left[ z_{i,k}(x_{j(i,k)} - t_{i,k}) \right]_{tr}^{q} = 0, \quad \textit{Otherwise} \tag{56}$$

Here each function is considered as piecewise linear with a trained knot '$tr$' at each $x_{(i,k)}$. By allowing the basis function to bend at the knots, MARS can model functions that differ in behaviour over the domain of each variable. This is applied to interaction terms as well. The interactions are no longer treated as global across the entire range of predictors but between the sub-regions of every basis function generated. Depending on fitment, the maximum number of knots to be considered, the minimum number of observations between knots, and the highest order of interaction terms are determined. The screening of automated variables occur as a result of using a modification of the generalized cross-validation (GCV) model fit criterion, developed by Craven and Wahba [136]. MARS finds the location and number of the needed spline basis functions in a forward or backward stepwise fashion. It starts by over-fitting a spline function through each knot, and then by removing the knots that least contribute to the overall fit of the model as determined by the modified GCV criterion, often completely removing the most insignificant variables. The equation depicting the lack-of-fit ($L_f$) criterion used by MARS as

$$L_f(Y_{\tilde{k}}) = G_{cv}(\tilde{k}) = \frac{\frac{1}{n}\sum_{i=1}^{n} [Y_i - Y_{\tilde{k}}(x_i)]^2}{\left[1 - \frac{\tilde{c}(\tilde{k})}{n}\right]^2} \tag{57}$$

where $\tilde{c}(\tilde{k}) = c(\tilde{k}) + M \cdot \tilde{k}$

where '$n$' denotes the number of sample observations, $\tilde{c}(\tilde{k})$ is the number of linearly independent basis functions, $\tilde{k}$ is the number of knots selected in the forward process, and '$M$' is a cost for basis-function optimization as well as a smoothing parameter for the procedure. The larger values of '$M$' result in fewer knots and smoother function estimates. The best MARS approximation is the one with the highest GCV value. Thus MARS is also compared with parametric and nonparametric approximation routines in terms of its accuracy, efficiency, robustness, model transparency, and simplicity and it is found suitable methodologies because it is more interpretable than most recursive partitioning, neural and adaptive strategies wherein it distinguishes well between actual and noise variables. Compared to other techniques, the use of MARS for engineering design applications is relatively new. Sudjianto et al. [137] use MARS to emulate a conceptually intensive complex automotive shock tower model in fatigue life durability analysis. Wang et al. [138], compare MARS to linear, second-order, and higher-order regression models for a five variable automobile structural analysis. Friedman [135] uses the MARS procedure to approximate behaviour of performance variables in a simple alternating current series circuit. The major advantages of using the MARS procedure appears to be accuracy and major reduction in computational cost associated with constructing the metamodel compared to the kriging method.

### 3.6. Radial basis function (RBF)

Quadratic surrogates have the benefit of being easy to implement while still being able to model curvature of the underlying function. Another way to model curvature is to consider interpolating surrogates, which are linear combinations of nonlinear basis functions and satisfy the interpolation points. RBF is often used to perform the interpolation of scattered multivariate data [139–141]. The metamodel appears in a linear combination of Euclidean distances can be expressed as

$$\hat{Y}(x) = \sum_{k=1}^{n} w_k \phi_k(X, x_k) \tag{58}$$

where, $n$ is the number of sampling points, $w_k$ is the weight determined by the least-squares method and $\phi_k(X, x_k)$ is the $k$th basis function determined at the sampling point $x_k$. Various symmetric radial functions are used as the basis function. The radial function for RBF model can be expressed as,

$$R_f(x) = \exp\left( -\frac{(x-c)^T(x-c)}{r^2} \right) \quad \text{(For Gaussian)} \tag{59}$$

$$R_f(x) = \sqrt{1 + \frac{(x-c)^T(x-c)}{r^2}} \quad \text{(For multi-quadratic)} \tag{60}$$

$$R_f(x) = \frac{1}{\sqrt{1 + \frac{(x-c)^T(x-c)}{r^2}}} \quad \text{(For inverse multi-quadratic)} \tag{61}$$

$$R_f(x) = \frac{1}{1 + \frac{(x-c)^T(x-c)}{r^2}} \quad \text{(For Cauchy)} \tag{62}$$

The RBF method can be treated to be as an interpolator like Kriging. However, such an interpolation method has shortcomings in that the appearance of a metamodel varies significantly with the type of basis function and its internal parameters. In the present study, a Gaussian basis function is employed with the fixed parameter $r^2 = 1$. It should be noted that an RBF passes through all the sampling points exactly. This means that function values from the approximate function are equal to the true function values at

the sampling points. This can be seen from the way that the coefficients are found. Therefore, it would not be possible to check RBF model fitness with ANOVA, which is a drawback of RBF.

### 3.7. Moving least squares (MLS)

In general, the polynomial regression models give the large errors in conjunction to non-linear responses while give good approximations in small regions wherein the responses are less complex. Such features are found advantageous while implementing the method of moving least squares (MLS). Moreover, the least square method gives a good result to represent the original limit state but it creates a problem if anyone like to fit a highly nonlinear limit function with this technique because this technique uses same factor for approximation throughout the space of interest. To overcome this problem, the moving least square method is introduced. In this method, a weighted interpolation function or limit state function is employed to the response surface and some extra support points are also generated over least square method to represent perfectly the nonlinear limit surface. In stochastic analysis, uncertainties can be expressed as a vector of random variables, $x = [x_1, x_2, x_3, \ldots x_n]^T$, characterized by a probability density function (PDF) with a particular distribution such as normal or log-normal with limit state function of these random variables. To avoid the curse of dimensionality in dealing with random input variables, response surface methods (RSM) can be utilised to increase the computational efficiency. These methods approximate an implicit limit state function as a response surface function (RSF) in an explicit form, which is evaluated for a set of selected design points throughout a number of deterministic structural analyses. RSM approximates an implicit limit state function as a RSF in explicit form. It selects experimental points by an axial sampling scheme and fits these experimental points using a second order polynomial without cross terms expressed as

$$y(x) = \beta_o + \sum_{i=1}^{k}\beta_i x_i + \sum_{i=1}^{k}\sum_{j>i}^{k}\beta_{ij}x_i x_j + \sum_{i=1}^{k}\beta_{ii}x_i^2 \tag{63}$$

where $\beta_o, \beta_i, \beta_{ij}$ and $\beta_{ii}$ are the unknown coefficients of the polynomial equation. The least squares approximation commonly used in the conventional RSM allots equal weight to the experimental points in evaluating the unknown coefficients of the RSF. The weights of these experimental points should consider the proximity to the actual limit state function so that MLS [142–144] enables a higher weight to yield a more accurate output. The approximated RSF can be defined in terms of basis functions $b(x)$ and the coefficient vector $a(x)$ as

$$\tilde{L}(x) = b(x)^T a(x) \tag{64}$$

The coefficient vector $a(x)$ is expressed as a function of the random variables x to consider the variation of the coefficient vector according to the change of the random variable at each iteration. The local MLS approximation at $x$ is formulated as [20]

$$\tilde{L}(x, x_i) = b(x_i)^T a(x) \tag{65}$$

where $x_i$ denotes experimental points and the basis functions $B(x)$ are commonly chosen as

$$b(x) = \left[1 x_1 \ldots x_n x^2 \ldots x_n^2\right]^T \tag{66}$$

The vector of unknown coefficients $a(x)$ is determined by minimizing the error between the experimental and approximated values of the limit state function. This error is defined as

$$Err(x) = \sum_{i=1}^{n} w(x - x_i)\left[\tilde{L}(x, x_i) - L(x_i)\right]^2 = (Ba - L)^T W(x)(Ba - L) \tag{67}$$

where $L = [L(x_1), L(x_2), \ldots L(x_n)]^T$, $B = [b(x_1), b(x_2), \ldots b(x_n)]^T$ and $W(x) = diag.[w_1(x_1 - x), w_2(x_2 - x), \ldots w_m(x_n - x)]$.

Here $(n + 1)$ is the number of sampling points and $(m + 1)$ is the number of basis functions. Now for minimization of error with respect to $a(x)$, $\partial(Err)/\partial a = 0$ transforming the coefficient of vector $a(x)$ as

$$a(x) = (B^T W(x) B)^{-1} B^T W(x) L \tag{68}$$

The approximated response surface function is obtained from Eq. (65) as

$$\tilde{L}(x) = b(x)^T (B^T W(x) B)^{-1} B^T W(x) L \tag{69}$$

### 3.8. Group method of data handling – polynomial neural network (GMDH-PNN)

In general, the Polynomial Neural Network (PNN) algorithm [23,24] is the advanced succession of Group Method of Data Handling (GMDH) method wherein different linear, modified quadratic, cubic polynomials are used. By choosing the most significant input variables and polynomial order among various types of forms available, the best partial description ($PD$) can be obtained based on selection of nodes of each layer and generation of additional layers until the best performance is reached. Such methodology leads to an optimal PNN structure wherein the input–output data set can be expressed as

$$(X_i, Y_i) = (x_{1i}, x_{2i}, x_{3i}, \ldots x_{ni}, y_i) \quad \text{where } i, j = 1, 2, 3 \ldots n \tag{70}$$

By computing the polynomial regression equations for each pair of input variable $x_i$ and $x_j$ and output $Y$ of the object system which desires to modelling

$$Y = A + Bx_i + Cx_j + Dx_i^2 + Ex_j^2 + Fx_i x_j \quad \text{where } i, j = 1, 2, 3 \ldots n \tag{71}$$

where $A$, $B$, $C$, $D$, $E$, $F$ are the coefficients of the polynomial equation. This provides $n(n-1)/2$ high-order variables for predicting the output $Y$ in place of the original $n$ variables $(x_1, x_2, \ldots, x_n)$ After finding these regression equations from a set of input-output observations, we then find out which ones to save. This gives the best predicted collection of quadratic regression models. We now use each of the quadratic equations that we have just computed and generate new independent observations that will replace the original observations of the variables $(x_1, x_2, \ldots, x_n)$ From these new independent variables we will combine them exactly as we did before. That is, we compute all of the quadratic regression equations of $Y$ versus these new variables. This will provide a new collection of $n(n-1)/2$ regression equation for predicting $Y$ from the new variables, which in turn are estimates of $Y$ from above equations. Now the best of new estimates is selected to generate new independent variables from selected equations to replace the old, and combine all pair of these new variables. This process is continued until the regression equations begin to have a poorer predictability power than did the previous ones. In other words, it is the time when the model starts to become overfitted. The estimated output $\hat{Y}_i$ can be further expressed as

$$\begin{aligned}\hat{Y} &= \hat{f}(x_1, x_2, x_3, \ldots x_n) \\ &= A_0 + \sum_{i=1}^{n} B_i x_i + \sum_{i=1}^{n}\sum_{j=1}^{n} C_{ij} x_i x_j + \sum_{i=1}^{n}\sum_{j=1}^{n}\sum_{k=1}^{n} D_{ijk} x_i x_j x_k + \cdots \\ &\quad \text{where } i, j, k = 1, 2, 3 \ldots n\end{aligned} \tag{72}$$

where $X(x_1, x_2, \ldots, x_n)$ is the input variables vector and $P(A_0, B_i, C_{ij}, D_{ijk}, \ldots)$ is vector of coefficients or weight of the Ivakhnenko polynomials. Components of the input vector X can

be independent variables, functional forms or finite difference terms. This algorithm allows to find simultaneously the structure of model and model system output on the values of most significant inputs of the system. The following steps are to be performed for the framework of the design procedure of PNN [145]:

Step1: *Determination of input variables:* Define the input variables as $x_i = 1, 2, 3, \ldots n$ related to output variable $Y$. If required, the normalization of input data is also completed.

Step 2: *Create training and testing data*: Create the input–output data set $(n)$ and divide into two parts, namely, training data $(n_{train})$ and testing data $(n_{test})$ where $n = n_{train} + n_{test}$. The training data set is employed to construct the PNN model including an estimation of the coefficients of the partial description of nodes situated in each layer of the PNN. Next, the testing data set is used to evaluate the estimated PNN model.

Step 3: *Selection of structure*: The structure of PNN is selected based on the number of input variables and the order of *PD* in each layer. Two kinds of PNN structures, namely a basic PNN and a modified PNN structure are distinguished. The basic taxonomy for the architectures of PNN structure is furnished in Fig. 6.

Step 4: *Determination of number of input variables and order of the polynomial*: Determine the regression polynomial structure of a *PD* related to PNN structure. The input variables of a node from $n$ input variables $x_1, x_2, x_3, \ldots x_n$ are selected. The total number of *PD*s located at the current layer differs according to the number of the selected input variables from the nodes of the preceding layer. This results in $k = n!/(n! - r!)r!$ nodes, where $r$ is the number of the chosen input variables. The choice of the input variables and the order of a *PD* itself help to select the best model with respect to the characteristics of the data, model design strategy, nonlinearity and predictive capability.

Step 5: *Estimation of coefficients of PD*: The vector of coefficients $A_i$ is derived by minimizing the mean squared error between $Y_i$ and $\hat{Y}_i$ .

$$PI = \frac{1}{n_{train}} \sum_{i=1}^{n_{train}} (Y_i - \hat{Y}_i)^2 \tag{73}$$

where *PI* represents a criterion which uses the mean squared differences between the output data of original system and the output data of the model. Using the training data subset, this gives rise to the set of linear equations

$$Y = \sum_{i=1}^{n} X_i A_i \tag{74}$$

The coefficients of the *PD* of the processing nodes in each layer are derived in the form

$$A_i = [X_i^T X_i]^{-1} X_i^T Y \tag{75}$$

where

$$Y = [y_1, y_1, y_1, y_1, \ldots, y_{n_{train}}]^T$$

$$X_i = [x_{1i}, x_{2i}, x_{3i} \ldots X_{ki} \ldots X_{train\,i}]^T$$

$$X_{ki}^T = [x_{ki1} x_{ki2} \ldots x_{kin} \ldots x_{ki1}^m, x_{ki2}^m \ldots x_{kin}^m]^T$$

$$A_i = [A_{0i} A_{1i} A_{2i} \ldots A_{n'i}]^T$$

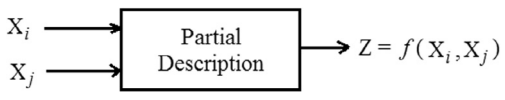


**Fig. 6.** Taxonomy for architectures of PNN.

with the following notations $i$ as the node number, $k$ as the data number, $n_{train}$ as the number of the training data subset, $n$ as the number of the selected input variables, $m$ as the maximum order, and $n'$ as the number of estimated coefficients. This procedure is implemented repeatedly for all nodes of the layer and also for all layers of PNN starting from the input layer and moving to the output layer.

Step 6: *Selection of PDs with the best predictive capability*: Each *PD* is estimated and evaluated using both the training and testing data sets. Then we compare these values and choose several PDs, which give the best predictive performance for the output variable. Usually a predetermined number $W$ of PDs is utilized.

Step 7: *Check the stopping criterion*: The stopping condition indicates that a sufficiently good PNN model is accomplished at the previous layer, and the modelling can be terminated. This condition reads as $PI_j > PI^*$ where $PI_j$ is a minimal identification error of the current layer whereas $PI*$ denotes a minimal identification error that occurred at the previous layer.

Step 8: *Determination of new input variables for the next layer*: If $PI_j$ (the minimum value in the current layer) has not been satisfied (so the stopping criterion is not satisfied), the model has to be expanded. The outputs of the preserved *PD*s serve as new inputs to the next layer.

### 3.9. Artificial neural network (ANN)

The fundamental processing element of ANN is an artificial neuron (or simply a neuron). A biological neuron receives inputs from other sources, combines them, generally performs a non-linear operation on the result, and then outputs the final result [146]. In the present study, the stochastic natural frequencies can be determined due to variability of input parameters. The ability of the ANNs, to recognize and reproduce the cause-effect relationships through training for the multiple input-output systems makes them efficient to represent even the most complex systems [147]. The main advantages of ANN as compared to response surface method (RSM) include:

a) ANN does not require any prior specification of suitable fitting function, and
b) It also has a universal approximation capability to approximate almost all kinds of non-linear functions including quadratic functions, whereas RSM is generally useful for quadratic approximations [148].

A multi-layer perceptron (MLP) based feed-forward ANN, which makes use of the back propagation learning algorithm, was applied for computational modelling. The network consists of an input layer, one hidden layer and an output layer. Each neuron acts firstly as a adding junction, summing together all incoming values. After that, it is filtered through an activation transfer function, the output of which is forwarded to the next layer of neurons in the network. The hyperbolic tangent was used as the transfer function for the input and hidden layer nodes. The reason behind employing the transfer function as logistic function or hyperbolic tangent (*tanh*) can be described as the logistic function generates the values nearer to zero if the argument of the function is substantially negative. Hence, the output of the hidden neuron can be made close to zero, and thus lowering the learning rate for all subsequent weights. Thus, it will almost stop learning. The *tanh* function, in the similar fashion, can generate a value close to -1.0, and thus will maintain learning. The algorithm used to train ANN in this study is quick propagation (QP). This algorithm is belonging to the gradient descent back-propagation. It has been reported in the literature that quick propagation learning algorithm can be adopted for the training of all the ANN models [149]. The performance of the ANNs

are statistically measured by the root mean squared error (*RMSE*), the coefficient of determination ($R^2$) and the absolute average deviation (AAD) obtained as follows:

$$RMSE = \sqrt{\frac{1}{n}\sum_{i=1}^{n}(Y_i - Y_{id})^2} \tag{76}$$

$$R^2 = 1 - \frac{\sum_{i=1}^{n}(Y_i - Y_{id})^2}{\sum_{i=1}^{n}(Y_{id} - Y_m)^2} \tag{77}$$

$$AAD = \left[\frac{1}{n}\sum_{i=1}^{n}\left|\frac{(Y_i - Y_{id})}{Y_{id}}\right|\right] \times 100 \tag{78}$$

where $n$ is the number of points, $Y_i$ is the predicted value, $Y_{id}$ is the actual value, and $Y_m$ is the average of the actual values.

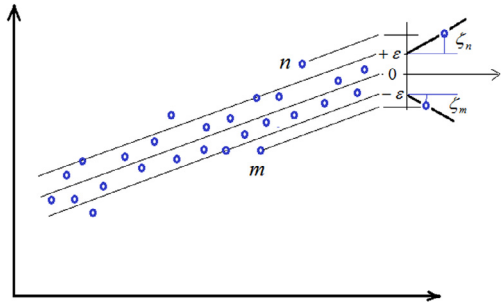


**Fig. 7.** Soft margin loss setting corresponding to a linear Support Vector machine.

### 3.10. Support vector regression method

Support vector regression (SVR) model is a special version of the Support Vector Machine (SVM) developed for regression analysis. Suppose the training data is given as $\{(x_1, y_1), (x_2, y_2) \ldots (x_l, y_l)\} \subset \chi \times \Re$ where $\chi$ and $\Re$ denote the space of the input patterns and Euclidean space vector. In support vector regression [150], the primary objective is to find a function $\hat{f}(x)$ that has at most $\varepsilon$ deviation from the actually obtained targets $y_i$ for all these training data and at the same time, is as flat as possible. In other words, errors are neglected as long as they are less than $\varepsilon$ (refer to Fig. 7), but it will not accept any deviation larger than this limiting value. Thus SVR model uses a subset of data samples, support vectors, to construct a metamodel that has a maximum deviation of $\varepsilon$ from the function value of each training data. For a linear regression, the SVR model can be written as

$$\hat{f}(x) = \hat{Y}(x) = \langle W \cdot x \rangle + b \tag{79}$$

where $\hat{Y}(x)$, $W$ and $b$ denote the approximate value of the objective function at $x$, vector of weights and the bias term, respectively while $\langle \cdot \rangle$ indicates the inner product. The sample points which lie within the $\pm\varepsilon$ band (known as the $\varepsilon$-tube) are ignored, with the predictor being defined entirely by those that lie on or outside this region termed as the support vectors. The basic form of the SVR prediction is the familiar sum of basis functions $\psi^{(i)}$, with weightings $w^{(i)}$, added to a base term $b$, which can be expressed as,

$$\hat{f}(x) = b + \sum_{i=1}^{k} W^{(i)} \psi(x, x^{(i)}) \tag{80}$$

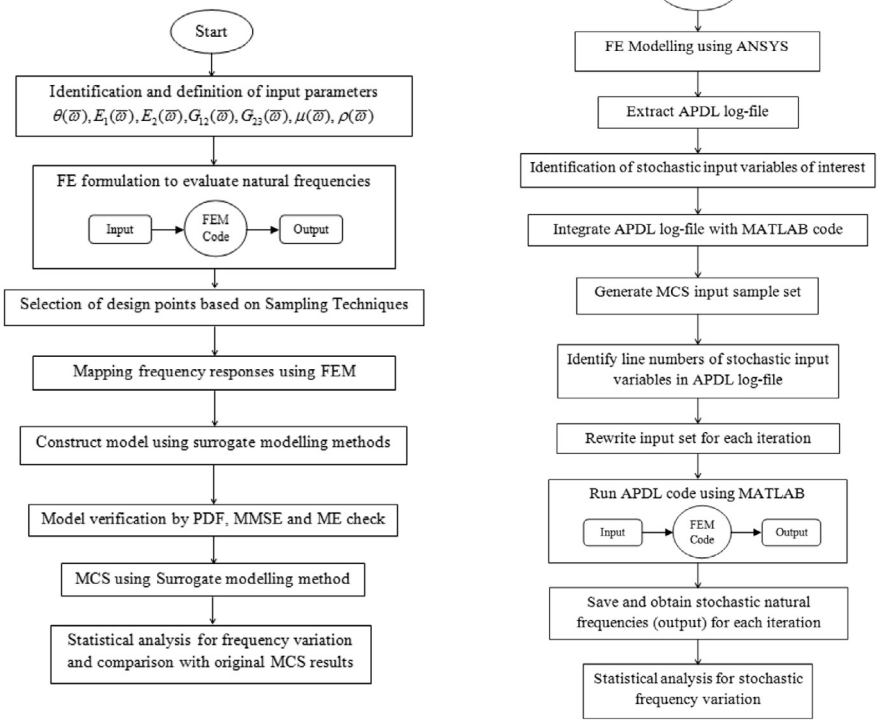


**Fig. 8.** Flowchart of stochastic natural frequency analysis using (a) surrogate model and (b) ANSYS.

**Table 2**
Convergence study for non-dimensional fundamental natural frequencies [$\omega = \omega_n L^2\sqrt{(\rho/E_1t^2)}$] of three layered (0°/−θ°/θ°) graphite-epoxy untwisted composite plates, $a/b = 1$, $b/t = 100$, considering $E_1 = 138$ GPa, $E_2 = 8.96$ GPa, $G_{12} = 7.1$ GPa, $\nu_{12} = 0.3$.

| Ply angle, θ | Methods | Mesh Sizes | | | | Qatu and Leissa [153] |
|---|---|---|---|---|---|---|
| | | 4 × 4 | 6 × 6 | 8 × 8 | 10 × 10 | |
| 0° | Present FEM | 1.0112 | 1.0133 | 1.0107 | 1.0040 | 1.0175 |
| | ANSYS | 1.0111 | 1.0130 | 1.0101 | 1.0035 | |
| 45° | Present FEM | 0.4591 | 0.4603 | 0.4603 | 0.4604 | 0.4613 |
| | ANSYS | 0.4588 | 0.4600 | 0.4598 | 0.4696 | |
| 90° | Present FEM | 0.2553 | 0.2567 | 0.2547 | 0.2542 | 0.2590 |
| | ANSYS | 0.2550 | 0.2565 | 0.2545 | 0.2541 | |

To produce a prediction which generalizes well, it is required to find the function with, at most, $\varepsilon$ deviations from y and at the same time, minimum complexity. Instead of minimizing the empirical risk on the training data during the fitting process, SVR minimizes an upper bound on the expected risk using an $\varepsilon$-insensitive loss function, as constrained convex quadratic optimization problem proposed by [42]

$$G(x) = \begin{cases} 0 & |Y(x) - \hat{Y}(x)| \leqslant \varepsilon \\ |Y(x) - \hat{Y}(x)| - \varepsilon & Otherwise \end{cases} \tag{81}$$

SVR model performs both linear as well as non-linear regression $\varepsilon$-insensitive loss function, at the same time, tries to reduce the model complexity by minimizing the norm of the weighting vector,

$$\text{Minimize } \frac{1}{2}||W||^2$$
$$\text{Subjected to } \begin{cases} Y_i - \langle W \cdot x^{(i)} \rangle - b \leqslant \varepsilon \\ \langle W \cdot x^{(i)} \rangle + b - Y_i \leqslant \varepsilon \end{cases} \tag{82}$$

It should be noted that there might not be a function that satisfies the condition in Eq. (82). The regularization parameter determines the trade-off between the model complexity and the degree for which deviation larger than $\varepsilon$ is tolerated in Eq. (82). A non-linear regression can be achieved by replacing the $\langle \cdot \rangle$ in Eq. (79) with a kernel function, $K$ as

$$\hat{f}(x) = \sum_{i=1}^{k} (\alpha_i - \alpha_i^*) K(x_i, x) + b \tag{83}$$

In the case studies examined in this paper, a Gaussian kernel function is used and $\varepsilon$ and $G$ parameters are chosen based on the recommendation proposed by Cherkassky and Ma [151]. For more details on SVR, the interested reader may refer to [150–152].

## 4. Metamodel based stochastic natural frequency analysis

The stochasticity in layer-wise material properties of laminated composite plates, such as longitudinal elastic modulus, transverse elastic modulus, longitudinal shear modulus, transverse shear modulus, Poisson's ratio, mass density and geometric properties such as ply-orientation angle are considered as input parameters. In the present study, frequency domain feature (first three natural frequencies) is considered as output. It is assumed that the distribution of randomness of input parameters exists within a certain band of tolerance with their central deterministic mean values following a uniform random distribution. Both individual (ply-orientation angle) and combined layer-wise variation of input parameters are considered to account for the effect of low and high dimensional input parameter space in the surrogate based uncertainty quantification algorithms as follows

(a) Variation of ply-orientation angle only:*** $\theta(\bar{\omega}) = \theta_1\theta_2\theta_3 \ldots \theta_i \ldots \theta_l$

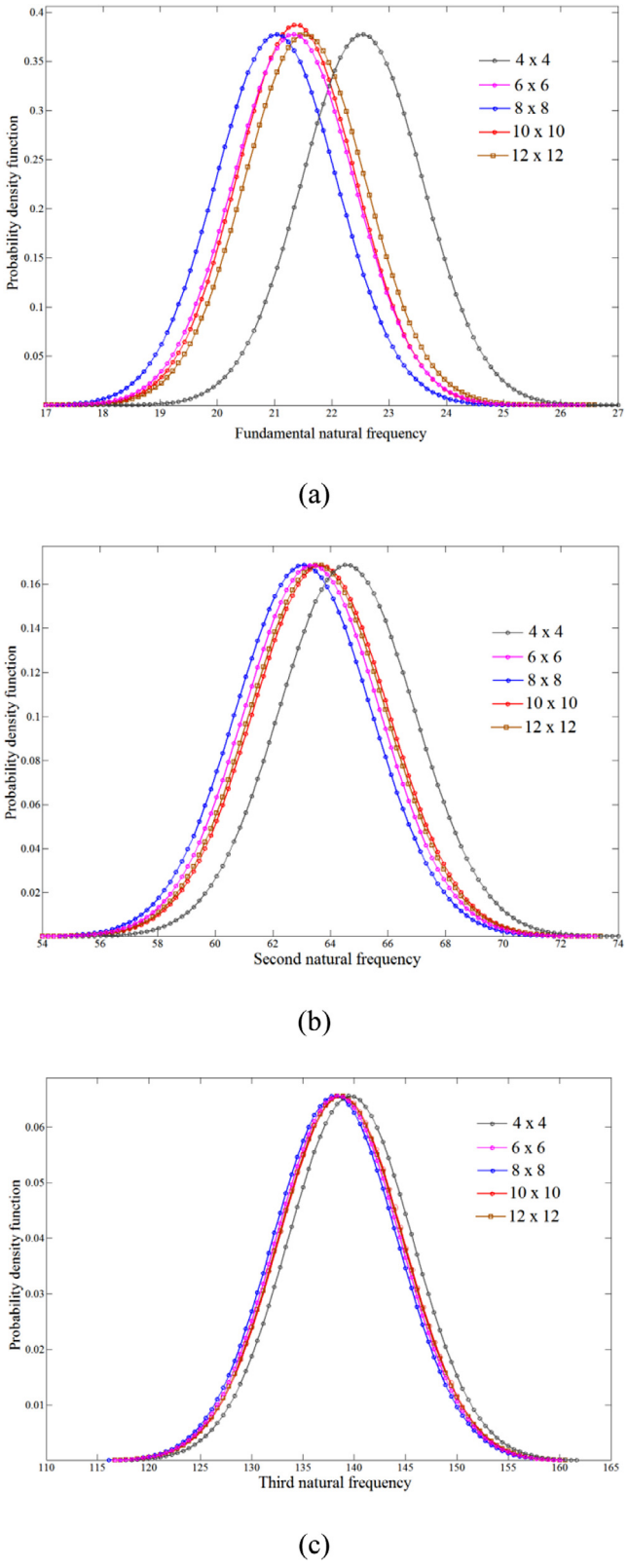


**Fig. 9.** Finite element mesh convergence study using ANSYS for combined stochasticity.

(b) Combined variation of ply orientation angle, elastic modulus (longitudinal and transverse), shear modulus (longitudinal and transverse), Poisson's ratio and mass density:

$$g\{\theta(\bar{\omega}),\rho(\bar{\omega}),G_{12}(\bar{\omega}),G_{23}(\bar{\omega}),E_1(\bar{\omega})\} = \{\Phi_1(\theta_1 \dots \theta_l),\Phi_2(E_{1(1)} \dots E_{1(l)}),\Phi_3(E_{2(1)} \dots E_{2(l)}),\Phi_4(G_{12(1)} \dots G_{12(l)}),\Phi_5(G_{23(1)} \dots G_{23(l)}),\Phi_6(\mu_1 \dots \mu_l),\Phi_7(\rho_1 \dots \rho_l)\}$$

where $\theta_i$, $E_{1(i)}$, $E_{2(i)}$, $G_{12(i)}$, $G_{23(i)}$, $\mu_i$ and $\rho_i$ are the ply orientation angle, elastic modulus along longitudinal and transverse direction, shear modulus along longitudinal direction, shear modulus along transverse direction, Poisson's ratio and mass density, respectively and '*l*' denotes the number of layer in the laminate. In present study, ±5° for ply orientation angle with subsequent ±10% tolerance for material properties from deterministic mean value are considered following standard industry practise for presenting results. The sampling technique for a particular surrogate modelling method is chosen on the basis of available literature to ensure best possible performance of each surrogate as furnished in Fig. 3. Fig. 8(a) presents the flowchart of stochastic natural frequency analysis using surrogate models.

A major limitation of the studies on uncertainty quantification of laminated composites as presented in the literature review section is that most of the investigations are based on finite element codes written in scientific programming languages like FORTRAN or MATLAB. This restricts application of such uncertainty quantification methods to large-scale complex structures, for which commercially available finite element modelling packages are commonly used in industry. In this article, we present a useful industry oriented uncertainty quantification scheme using commercial finite element software in conjunction with MATLAB. For that purpose, the APDL script generated after modelling the composite plate in ANSYS environment is integrated with MATLAB. A fully automated MATLAB code is developed capable of rewriting the APDL script in each iteration containing the random values of stochastic input parameters, then running the APDL script to obtain desired outputs (refer the flowchart presented in Fig. 8(b)) and saving the results for each sample. Thus Monte Carlo simulation can be carried out using ANSYS in conjunction with MATLAB for any number of samples following the proposed approach.

## 5. Results and discussion

The previous investigations in the field of laminated composites have focused on the deterministic aspect of different static and dynamic responses over the last few decades [153–169]. A relatively new area of research is the quantification of uncertainty in laminated composite structures [170]. The amount of research carried out in the field of uncertainty quantification of composite structures is insufficient owing to the computational intensiveness of such analyses. However, the stage of research on application of metamodels to achieve computational efficiency in the uncertainty

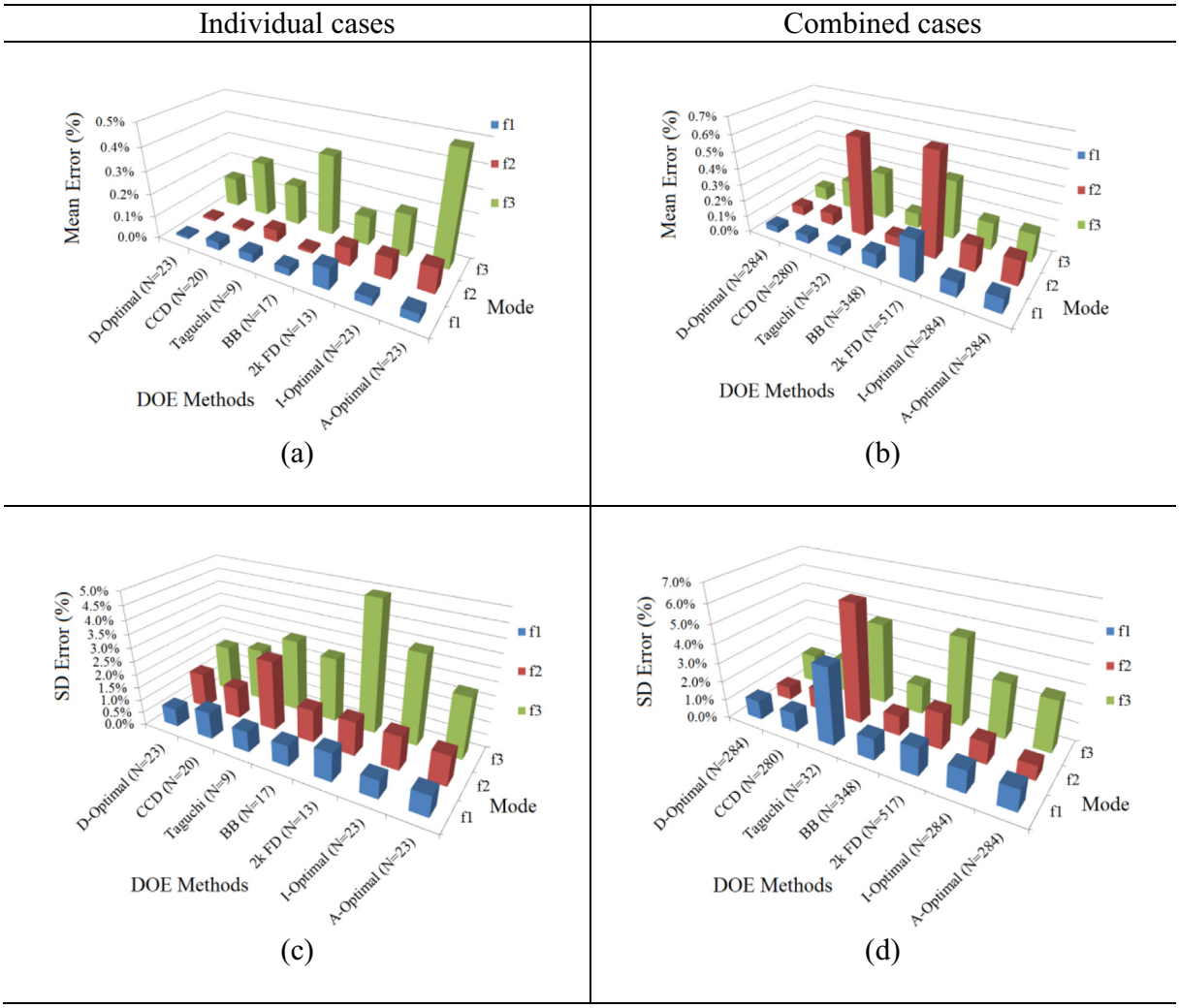


**Fig. 10.** (a–d) Error (%) of mean and standard deviation of first three natural frequencies between polynomial regression method with different design of experiment methods and MCS results for individual variation of ply orientation angle and combined variation ($f_1$ $f_2$ and $f_3$ denote first three modes of vibration).

quantification of composites is still in its infancy. As discussed in the introduction section, all the investigations on metamodel based uncertainty quantification of laminated composites are performed using a single metamodel. Thus there exists a strong rationale among the scientific community to investigate the relative performance of different metamodels, which is the focus of the present study. In the present paper, a three layered graphite-epoxy symmetric angle-ply (45°/−45°/45°) laminated composite cantilever plate is considered to investigate the comparative performance of different metamodels on the basis of accuracy and computational efficiency. The length, width and thickness of the composite laminate considered in the present analysis are 1 m, 1 m and 5 mm, respectively. Material properties of graphite–epoxy composite [171] considered with deterministic mean value as $E_1 = 138.0$ GPa, $E_2 = 8.96$ GPa, $G_{12} = 7.1$ GPa, $G_{13} = 7.1$ GPa, $G_{23} = 2.84$ GPa, $\mu = 0.3$, $\rho = 3202$ kg/m$^3$. An eight noded isoparametric quadratic plate bending element is considered for the present FEM approach. For full scale MCS, number of original finite element analysis is same as the sampling size. In general for complex composite structures, the performance function is not available as an explicit function of the random design variables. The considered metamodels are employed to find the predictive and representative surrogates relating the first three natural frequencies to a number of input variables on a comparative basis. Thus the metamodels are used to determine the first three natural frequencies corresponding to given values of stochastic input variables, instead of time-consuming and computationally intensive finite element analysis.

Table 2 presents the finite element mesh convergence study for non-dimensional fundamental natural frequencies of three layered graphite-epoxy untwisted composite plates validated with the results obtained from ANSYS as well as Quatu and Leissa [153]. Validation of the developed deterministic finite element code with the results of commercial packages like ANSYS caters to more confidence in the present analysis. Other than validation of the deterministic finite element formulation by computer code, ANSYS is also employed to validate the stochastic model of three layered angle-ply (45°/−45°/45°) composite cantilever plates corresponding to individual and combined variation of input parameters following the algorithm presented in Fig. 8(b). A convergence study is carried out with respect to mesh sizes (4 × 4), (6 × 6), (8 × 8), (10 × 10) and (12 × 12) as furnished in Fig. 9. To enumerate best predictive mesh convergence, (6 × 6) mesh size is considered in the present comparative study corresponding to individual and combined variation of input parameters.

A comparative assessment of different design of experiment methods has been carried out in conjunction with polynomial regression method. Fig. 10 presents the error in percentage of mean and standard deviation of first three natural frequencies for polynomial regression based stochastic analysis using different design of experiment algorithms with respect to MCS results for individual variation of ply orientation angle $\{\theta(\bar{\omega})\}$ and combined variation $\{\theta(\bar{\omega}), E_1(\bar{\omega}), E_2(\bar{\omega}), G_{12}(\bar{\omega}), G_{23}(\bar{\omega}), \mu(\bar{\omega}), \rho(\bar{\omega})\}$. D-optimal design method is observed to be the most computationally efficient and accurate compared to other design of experiment algorithms. The scatter plot and probability density function plot for first three natural frequencies corresponding to combined variation of input parameters are furnished in Fig. 11 considering polynomial regression using D-optimal design method along with traditional Monte Carlo simulation results. The figures corroborate excellent capability of D-optimal design based polynomial regression method in prediction as well as characterizing the probabilistic features for first three natural frequencies.

Fig. 12 presents the percentage error of mean and standard deviation of first three natural frequencies between the considered surrogate modelling methods and MCS results with respect to different sample sizes for individual variation of ply orientation angle $[\theta(\bar{\omega})]$,while Fig. 13 indicates the error in percentage for mean and standard deviation of first three natural frequencies between surrogate modelling methods and MCS results with respect to

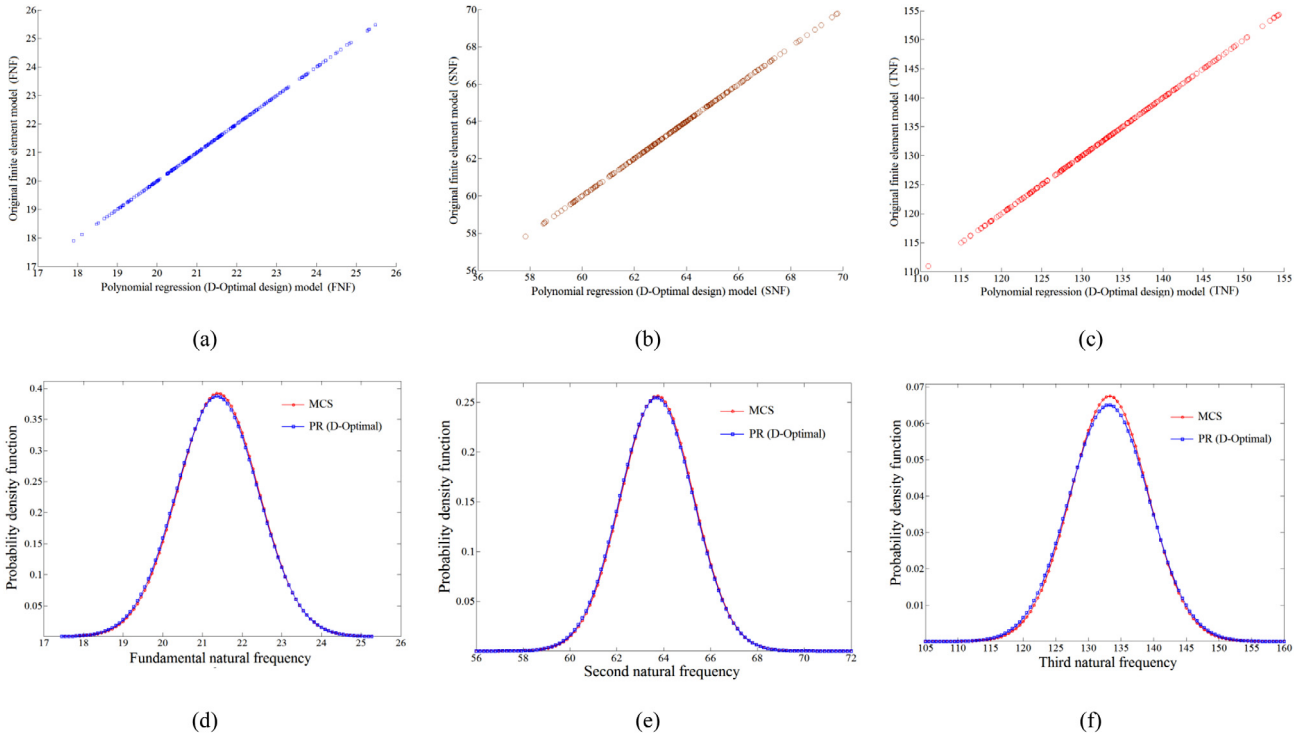


**Fig. 11.** Scatter diagram and probability density function for first three natural frequencies corresponding to combined variation of input parameters considering polynomial regression using D-optimal design method.

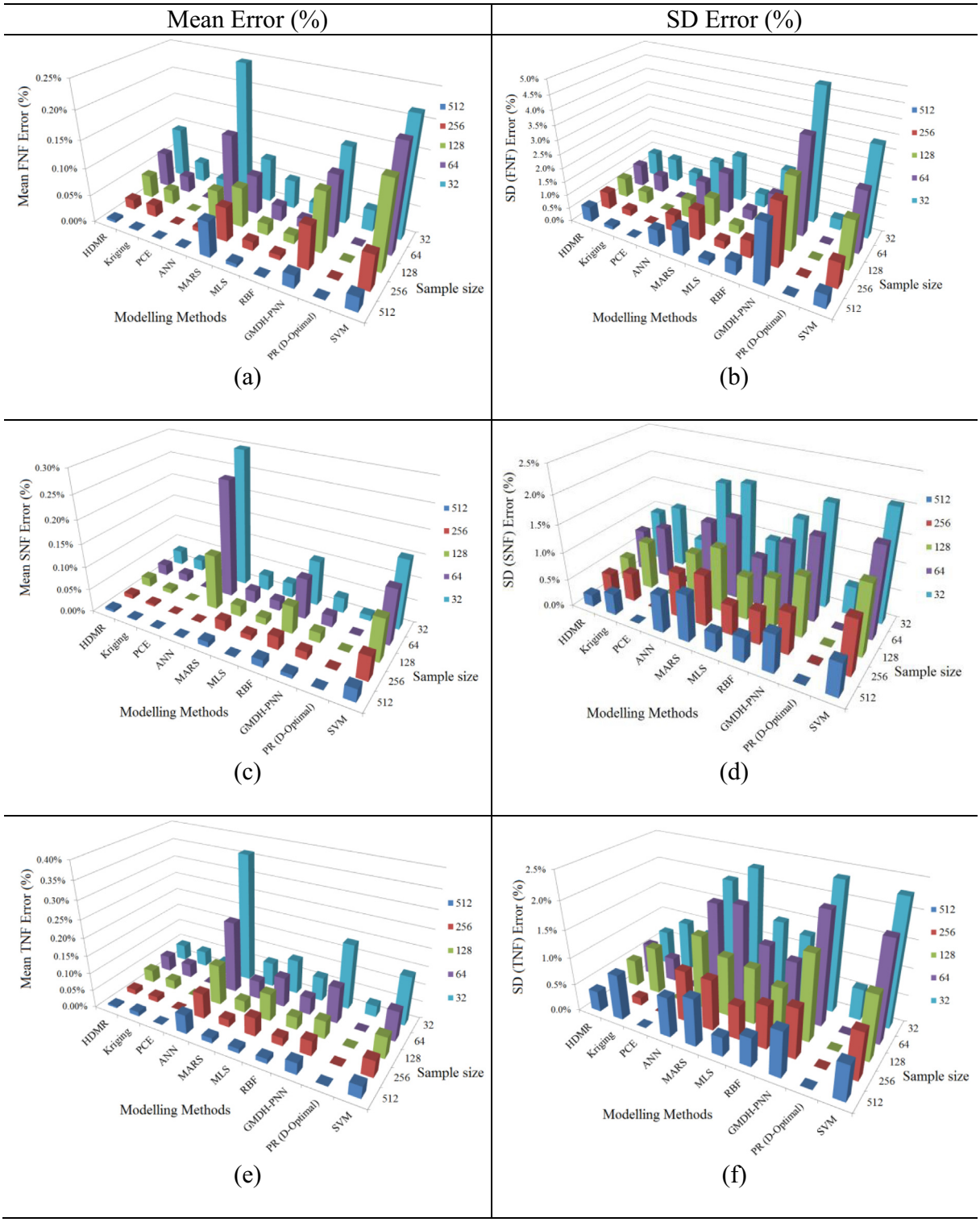


**Fig. 12.** (a–f) Error (%) of mean and standard deviation of first three natural frequencies between surrogate modelling methods and MCS results with respect to different sample sizes for individual variation of ply orientation angle [$\theta(\bar{\omega})$] for angle-ply (45°/−45°/45°) composite plates.

different sample sizes for combined variation of all stochastic input parameters $\{\theta(\bar{\omega}), E_1(\bar{\omega}), E_2(\bar{\omega}), G_{12}(\bar{\omega}), G_{23}(\bar{\omega}), \mu(\bar{\omega}), \rho(\bar{\omega})\}$. In general, for all cases, the sparsity of first three natural frequencies for combined variation of input parameters are found to be higher than that of individual variation of input parameter, as expected. As the sample size increases, the percentage of error of mean and standard deviation of first three natural frequencies between surrogate modelling methods and MCS results are found to reduce irrespective of modelling methods. An exhaustive study is carried out to enumerate the best minimum sample size required to construct the metamodel for all tested modelling methods corresponding to suitable sampling techniques. Polynomial regression

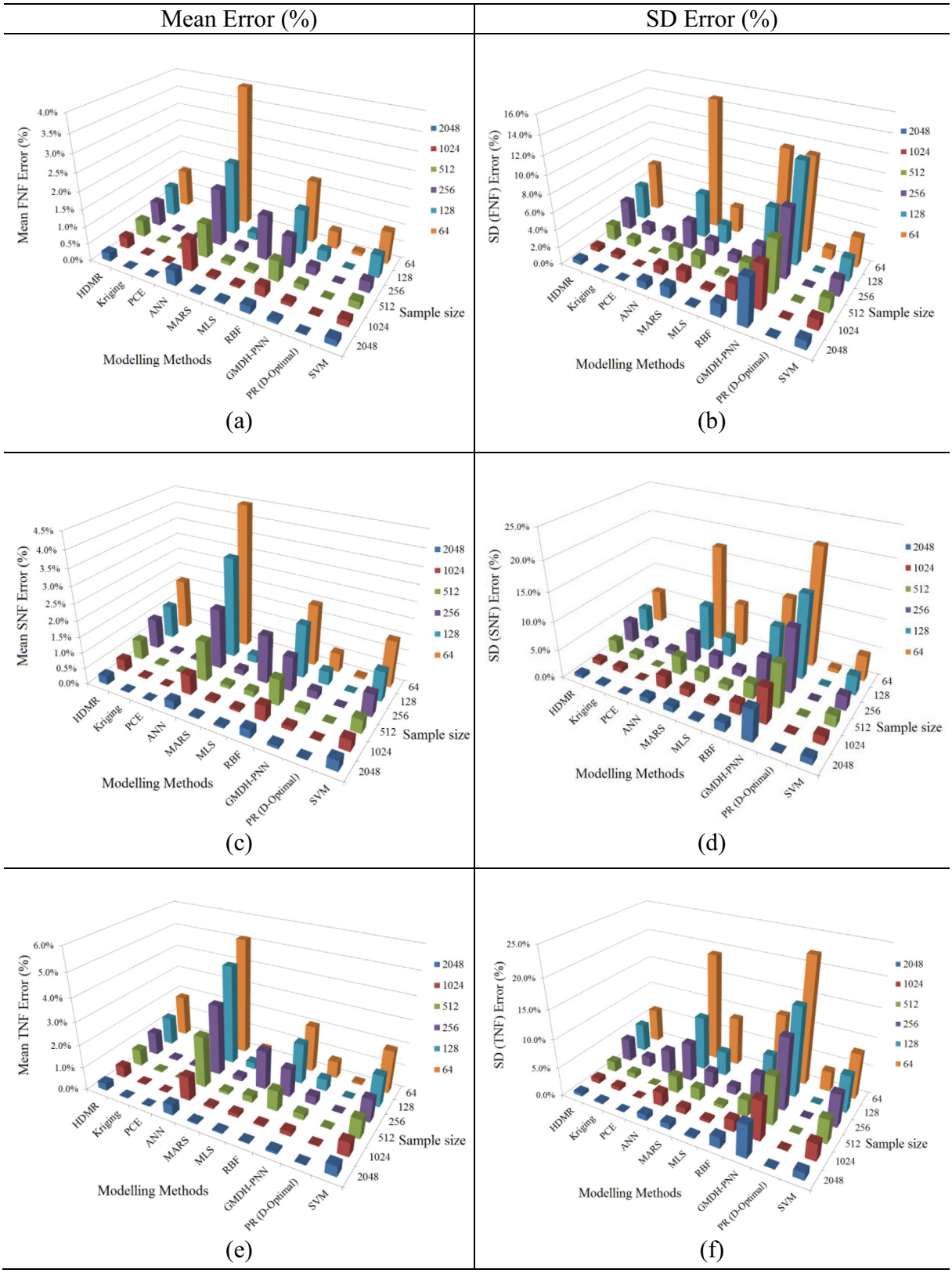


**Fig. 13.** (a–f) Error (%) of mean and standard deviation of first three natural frequencies between surrogate modelling methods and MCS results with respect to different sample sizes for combined variation $\{\theta(\bar{\omega}), E_1(\bar{\omega}), E_2(\bar{\omega}), G_{12}(\bar{\omega}), G_{23}(\bar{\omega}), \mu(\bar{\omega}), \rho(\bar{\omega})\}$ for angle-ply (45°/-45°/45°) composite plates.

with D-optimal design method is found to require least number of samples for suitable fitment of surrogates corresponding to individual as well as combined variation cases. In contrast, Group method of data handling – Polynomial neural network (GMDH-PNN) method and Support Vector Regression (SVR) are observed to require maximum number of sample for individual variation

while Artificial neural network (ANN) method is found to need the maximum number of samples for combined variation compared to other tested modelling methods. Table 3 presents the minimum number of samples required for different tested metamodelling methods to obtain reasonable accuracy in terms of mean and standard deviation for the layer-wise stochastic analysis of composite plate for both individual and combined variation. A clear idea about the performance of different metamodeling techniques from the viewpoint of computational efficiency can be perceived for both low and relatively higher dimensional input parameter space. The probability distributions obtained by using ten different metamodelling methods along with traditional MCS for first three natural frequencies corresponding to individual (only ply angle) and combined variation of input parameters are shown in Figs. 14 and 15, respectively. From the viewpoint ofaccuracy in probabilistic characterization with respect to traditional MCS, performances are comparatively worse for ANN and SVM in case of individual stochasticity and SVM and PCE in case of combined stochasticity respectively. Other metamodels are found to obtain satisfactory results, polynomial regression based on D-optimal design being the best. ANN performs better for the higher dimensional input parameter space (combined case), even though it requires more samples compared to most of the other methods. However, it can be noted that the results presented in Figs. 14–15 are obtained using the corresponding sample size provided in Table 3, which is finalized on the basis of error analysis for mean and standard deviation. The trade-off between desired level of accuracy and computational efficiency should be judged based on specific requirements for a particular problem. The results presented in this article along with the in-depth previous comparative investigations on response surface method [46] and kriging model variants [14] can provide a reasonably composed guideline for choosing sampling method and surrogate modelling technique for future applications. However, it should always be noted that surrogate modelling being a problem-specific technique, it is quite difficult to identify a single surrogate model that works best for all problems. Thus future researches are necessary to investigate the comparative performances of different surrogates for other types of problems in structural mechanics from different other angles such as non-linearity, dimension of input parameter space and the effect of correlation among them, noise etc. The present article will serve as an important reference for such future investigations.

**Table 3**
Minimum sample size required for different metamodeling methods.

| Sl. No. | Metamodeling methods | Mínimum number of samples required for model formation | |
|---|---|---|---|
| | | Individual variation | Combined variation |
| 1. | High dimensional model representation (HDMR) | 256 | 512 |
| 2. | Kriging method | 128 | 256 |
| 3. | Polynomial chaos expansion (PCE) | 64 | 128 |
| 4. | Artificial neural network (ANN) | 256 | 2048 |
| 5. | Multivariate adaptive regression splines (MARS) | 64 | 128 |
| 6. | Moving Least Square (MLS) | 128 | 512 |
| 7. | Radial basis function (RBF) | 64 | 1024 |
| 8. | Group method of data handling – Polynomial neural network (GMDH-PNN) | 512 | 1024 |
| 9. | Polynomial Regression (by D-optimal) | 32 | 64 |
| 10. | Support Vector Regression (SVR) | 512 | 1024 |

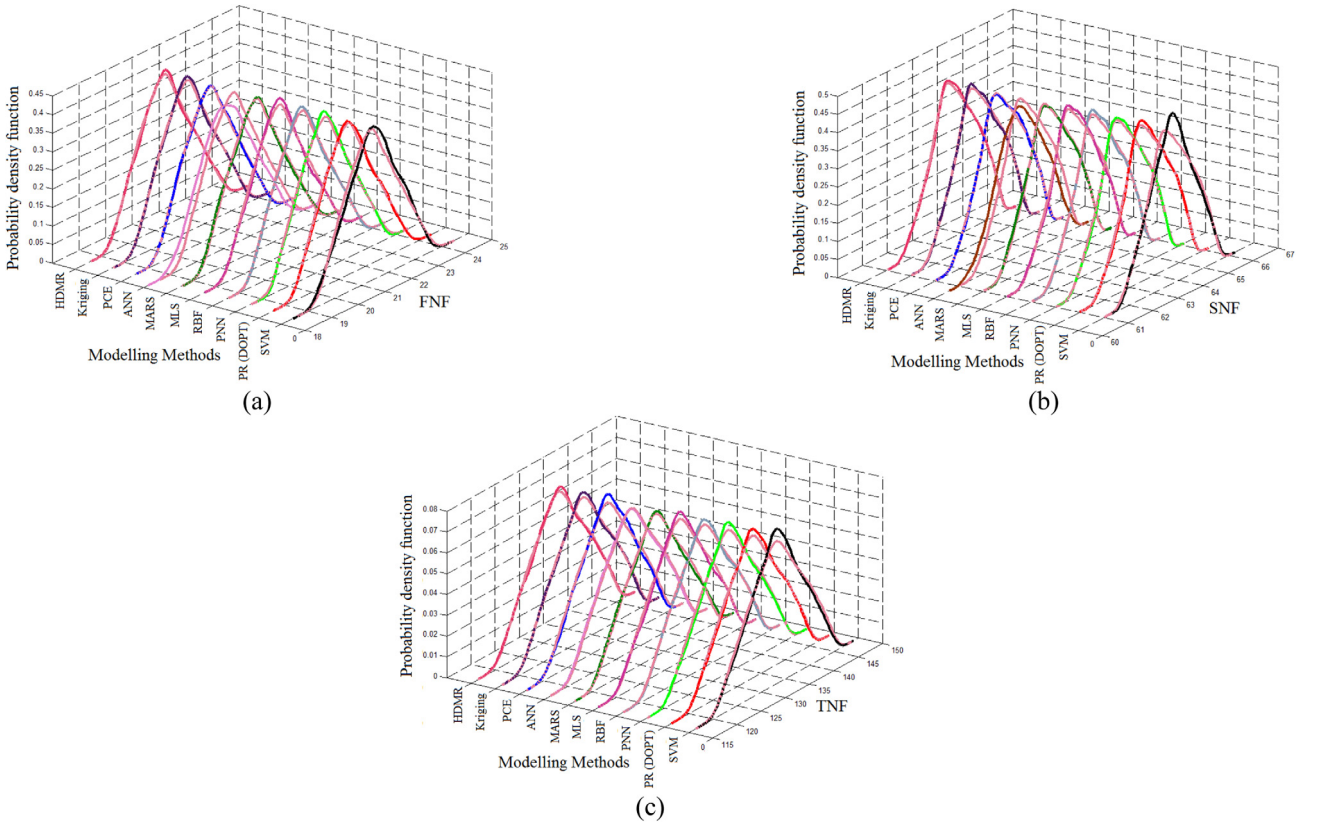


**Fig. 14.** Probability density function for first three natural frequencies corresponding to individual variation of input parameters (colour code: MCS and specification of other colours are indicated in the figures).

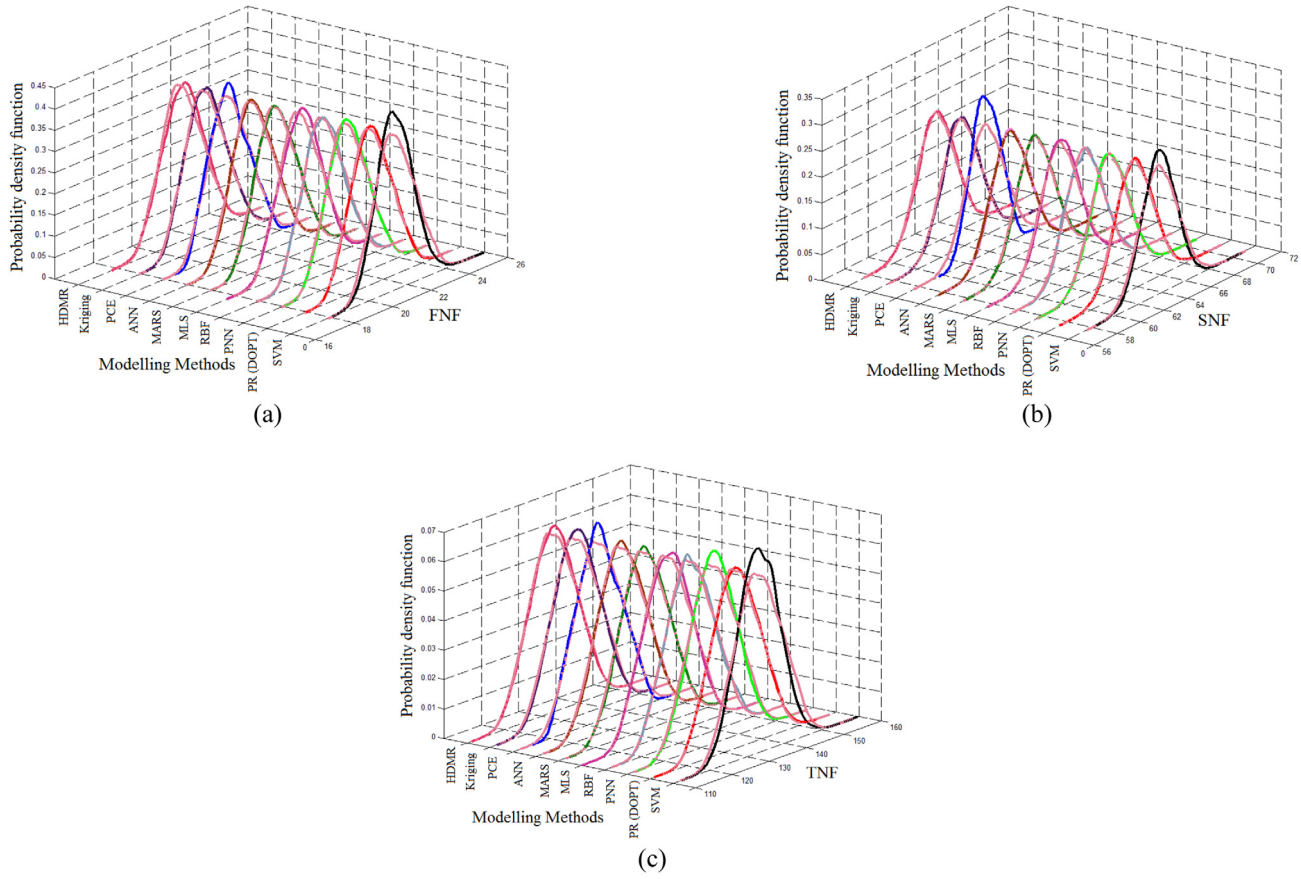


**Fig. 15.** Probability density function for first three natural frequencies corresponding to combined variation of input parameters (colour code: MCS and specification of other colours are indicated in the figures).

## 6. Conclusion

This paper presents a concise review on metamodel based uncertainty quantification algorithms along with a critical comparative assessment of different metamodels (such as polynomial regression, kriging, high dimensional model representation, polynomial chaos expansion, artificial neural network, moving least square, support vector regression, multivariate adaptive regression splines, radial basis function and polynomial neural network) for stochastic natural frequency analysis of composite laminates from the viewpoint of accuracy (with respect to traditional Monte Carlo simulation) and computational efficiency. To the best of authors' knowledge, this is the first ever attempt to present a comprehensive comparative investigation considering all the most prominent metamodeling techniques in such large scale providing a complete understanding about the relative performances based on different criteria. First three stochastic natural frequencies of a laminated composite plate are considered for individual and combined variation of layer-wise random input parameters. A comparative investigation is presented on different design of experiment methods (such as $2^k$ factorial designs, central composite design, A-Optimal design, I-Optimal, D-Optimal, Taguchi's orthogonal array design, Box-Behnken design) in conjunction with polynomial regression revealing that D-optimal design obtains most satisfactory results compared to others. For each of the metamodeling techniques, the rate of convergence with respect to traditional Monte Carlo simulation has been studied considering both low and high dimensional input parameter space. Probabilistic descriptions of the natural frequencies obtained on the basis of different metamodeling techniques are presented along with crude Monte Carlo simulation results.

Polynomial regression with D-optimal design method is found to be most computationally cost effective for suitable fitment of surrogates corresponding to individual as well as combined variation of input parameters. Group method of data handling – polynomial neural network (GMDH-PNN) method and support vector regression (SVR) are observed to be least computationally efficient for individual variation while artificial neural network (ANN) method is found to be most computationally expensive for combined variation compared to other metamodels. From the viewpoint of accuracy in probabilistic characterization with respect to traditional MCS, performances are comparatively worse for ANN and SVM in case of individual stochasticity while SVM and PCE shows relatively less accuracy in case of combined stochasticity. On the basis of the stochastic results presented in this article, a clear idea about the performance of different metamodeling techniques from the viewpoint of accuracy and computational efficiency can be perceived for both low and relatively higher dimensional input parameter space. Although this study focuses on stochastic natural frequency analysis of composite plates, the outcomes regarding comparative performance of different metamodels will serve as a valuable reference for different other computationally intensive problems in the broader field of science and engineering.

## Acknowledgements

TM acknowledges the financial support from Swansea University through the award of Zienkiewicz Scholarship during the period of this work. SA acknowledges the financial support from The Royal Society of London through the Wolfson Research Merit award.

## References


[1] Baran I, Cinar K, Ersoy N, Akkerman R, Hattel JH. A review on the mechanical modeling of composite manufacturing processes. Arch Comput Methods Eng 2016. http://dx.doi.org/10.1007/s11831-016-9167-2.

[2] Kleijnen JPC. Statistical tools for simulation practitioners. NY: Marcel Dekker; 1987.

[3] Arregui-Mena JD, Margetts L, Mummery PM. Practical application of the stochastic finite element method. Arch Comput Methods Eng 2016;23(1):171–90.

[4] Simpson TW, Peplinski J, Koch PN, Allen JK, On the use of statistics in design and the implications for deterministic computer experiments. Design Theory and Methodology – DTM'97 (held in Sacramento, CA), Paper No. DETC97/DTM-3881, ASME; 1997.

[5] Barthelemy Jean-François M, Haftka Raphael T. Approximation concepts for optimum structural design – a review. Struct Optim 1993;5(3):129–44.

[6] Sobieszczanski-Sobieski J, Haftka RT. Multidisciplinary aerospace design optimization: survey of recent developments. Struct. Optim. 1997;14:1–23.

[7] Dey TK, Mukhopadhyay T, Chakrabarti A, Sharma UK. Efficient lightweight design of FRP bridge deck. Proc Inst Civil Eng – Struct Build 2015;168(10):697–707.

[8] Mukhopadhyay T, Mahata A, Dey S, Adhikari S. Probabilistic analysis and design of HCP nanowires: an efficient surrogate based molecular dynamics simulation approach. J Mater Sci Technol 2016;32(12):1345–51.

[9] Myers RH, Montgomery DC. Response surface methodology: process and product optimization using designed experiments. New York, NY: John Wiley & Sons; 1995.

[10] Smith M. Neural networks for statistical modeling. NY: Von Nostrand Reinhold; 1993.

[11] Dey S, Mukhopadhyay T, Spickenheuer A, Gohs U, Adhikari S. Uncertainty quantification in natural frequency of composite plates – An Artificial neural network based approach. Adv Compos Lett 2016;25(2):43–8.

[12] Sacks J, Welch WJ, Mitchell TJ, Wynn HP. Design and analysis of computer experiments. Statist Sci 1989;4:409–35.

[13] Booker AJ, Dennis Jr JE, Frank PD, Serafini DB, Torczon V, Trosset MW. A rigorous framework for optimization of expensive functions by surrogates. Struct. Optim. 1999;17:1–13.

[14] Mukhopadhyay T, Chakraborty S, Dey S, Adhikari S, Chowdhury R. A critical assessment of Kriging model variants for high-fidelity uncertainty quantification in dynamics of composite shells. Arch Comput Methods Eng 2016. http://dx.doi.org/10.1007/s11831-016-9178-z.

[15] Friedman JH. Multivariate adaptive regression splines. Ann Stat 1991;19:1–141.

[16] Mukhopadhyay T, A multivariate adaptive regression splines based damage identification methodology for web core composite bridges including the effect of noise, J Sandwich Struct Mater, [in press].

[17] Naskar S, Mukhopadhyay T, Sriramula S, Adhikari S. Stochastic natural frequency analysis of damaged thin-walled laminated composite beams with uncertainty in micromechanical properties. Compos Struct 2017;160:312–34.

[18] Dyn N, Levin D, Rippa S. Numerical procedures for surface fitting of scattered data by radial basis functions. SIAM J Sci Stat Comput 1986;7:639–59.

[19] Youn BD, Choi Kyung K. A new response surface methodology for reliability-based design optimization. Comput Struct 2004;82:241–56.

[20] Kang Soo-Chang, Koh Hyun-Moo, Choo Jinkyo F. An efficient response surface method using moving least squares approximation for structural reliability analysis. Probab Eng Mech 2010;25:365–71.

[21] Hastie Trevor, Rosset Saharon, Tibshirani Robert, Zhu Ji. The entire regularization path for the support vector machine. J Mach Learn Res 2004;5:1391–415.

[22] Dai H, Zhang Boyi, Wang Wei. A multi wavelet support vector regression method for efficient reliability assessment. Reliab Eng Syst Saf 2015;136:132–9.

[23] Dey S, Naskar S, Mukhopadhyay T, Gohs U, Spickenheuer A, Bittrich L, et al. Uncertain natural frequency analysis of composite plates including effect of noise – A polynomial neural network approach. Compos Struct 2016;143:130–42.

[24] Mellit A, Drif M, Malek A. EPNN-based prediction of meteorological data for renewable energy systems. Revue des Energies Renouvelables 2010;13(1):25–47.

[25] Simpson TW, Mauery TM, Korte JJ, Mistree F. Comparison of response surface and kriging models for multidisciplinary design optimization. Proc. 7th AIAA/USAF/NASA/ISSMO Symp. on Multidisciplinary Analysis & Optimization (held in St. Louis, MO), vol. 1. AIAA; 1998. p. 381–91.

[26] Giunta A, Watson LT, Koehler J. A comparison of approximation modeling techniques: polynomial versus interpolating models. Proc. 7th AIAA/USAF/NASA/ISSMO Symp. on Multidisciplinary Analysis & Optimization (held in St. Louis, MO), vol. 1. p. 392–404. AIAA-98-4758.

[27] Varadarajan S, Chen W, Pelka C. The robust concept exploration method with enhanced model approximation capabilities. Eng. Opt. 2000;32:309–34.

[28] Yang RJ, Gu L, Liaw L, Gearhart C, Tho CH, Liu X, Wang BP. Approximations for safety optimization of large systems. ASME Design Automation Conf. (held in Baltimore, MD). Paper No. DETC-00/DAC-14245.

[29] Irisarri FX, Laurin F, Leroy FH, Maire JF. Computational strategy for multiobjective optimization of composite stiffened panels. Compos Struct 2011;93:1158–67.

[30] Rikards R, Abramovich H, Kalnins K, Auzins J. Surrogate modeling in design optimization of stiffened composite shells. Compos Struct 2006;73:244–51.

[31] Bisagni C, Lanzi L. Post-buckling optimisation of composite stiffened panels using neural networks. Compos Struct 2002;58:237–47.

[32] Liu B, Haftka RT, Akgün MA. Two-level composite wing structural optimization using response surfaces. Struct Multidiscipl Optim 2000;20:87–96.

[33] Lee YJ, Lin CC. Regression of the response surface of laminated composite structures. Compos Struct 2003;62:91–105.

[34] Lin CC, Lee YJ. Stacking sequence optimization of laminated composite structures using genetic algorithm with local improvement. Compos Struct 2004;63:339–45.

[35] Kalnins K, Rikards R, Auzins J, Bisagni C, Abramovich H, Degenhardt R. Metamodeling methodology for postbuckling simulation of damaged composite stiffened structures with physical validation. Int J Struct Stab Dyn 2010;10:705–16.

[36] Lanzi L, Giavotto V. Post-buckling optimization of composite stiffened panels: computations and experiments. Compos Struct 2006;73:208–20.

[37] Vandervelde T, Milani AS. Layout optimization of a multi-zoned, multi-layered composite wing under free vibration. Proceedings of SPIE, the international society for optical engineering San Diego, CA, USA.

[38] Blom AW, Stickler PB, Gürdal Z. Optimization of a composite cylinder under bending by tailoring stiffness properties in circumferential direction. Compos Part B Eng 2010;41:157–65.

[39] Arian Nik M, Fayazbakhsh K, Pasini D, Lessard L. Surrogate-based multiobjective optimization of a composite laminate with curvilinear fibers. Compos Struct 2012;94:2306–23.

[40] Arian Nik M, Fayazbakhsh K, Pasini D, Lessard L. Optimization of variable stiffness composites with embedded defects induced by Automated Fiber Placement. Compos Struct 2014;107:160–6.

[41] Fayazbakhsh K, Arian Nik M, Pasini D, Lessard L. Defect layer method to capture effect of gaps and overlaps in variable stiffness laminates made by automated fiber placement. Compos Struct 2013;97:245–51.

[42] Viana FAC, Gogu C, Haftka RT. Making the most out of surrogate models: tricks of the trade. ASME conference proceedings. p. 587–98.

[43] Chen W. A robust concept exploration method for configuring complex system Ph.D. Dissertation Thesis. Atlanta, GA: Mechanical Engineering, Georgia Institute of Technology; 1995.

[44] Mukhopadhyay T, Dey TK, Dey S, Chakrabarti A. Optimization of fiber reinforced polymer web core bridge deck – A hybrid approach. Struct Eng Int 2015;25(2):173–83.

[45] Dey S, Mukhopadhyay T, Khodaparast HH, Adhikari S. A response surface modelling approach for resonance driven reliability based optimization of composite shells. Periodica Polytechnica – Civil Eng 2016;60(1):103–11.

[46] Mukhopadhyay T, Dey TK, Chowdhury R, Chakrabarti A. Structural damage identification using response surface based multi-objective optimization: a comparative study. Arabian J Sci Eng 2015;40(4):1027–44.

[47] Sacks J, Welch WJ, Mitchell TJ, Wynn HP. Design and analysis of computer experiments. Stat Sci 1989;4(4):409–35.

[48] Jin R, Chen W, Simpson TW. Comparative studies of metamodeling techniques under multiple modeling criteria. Struct Multidiscip Optim 2001;23(1):1–13.

[49] Koehler JR, Owen A. Computer experiments. In: Ghosh S, Rao CR, editors. Handbook of statistics. New York: Elsevier Science; 1996. p. 261–308.

[50] Currin C, Mitchell TJ, Morris MD, Ylvisaker D. Bayesian prediction of deterministic functions, with applications to the design and analysis of computer experiments. J Am Stat Assoc 1991;86(416):953–63.

[51] Johnson ME, Moore LM, Ylvisaker D. Minimax and maximin distance designs. J Stat Plann Inferences 1990;26(2):131–48.

[52] Taguchi G, Yokoyama Y, Wu Y. Taguchi methods: design of experiments. Allen Park, Michigan: American Supplier Institute; 1993.

[53] Owen A. Orthogonal arrays for computer experiments, integration, and visualization. Statistical Sinica 1992;2:439–52.

[54] Hedayat AS, Sloane NJA, Stufken J. Orthogonal arrays: theory and applications. New York: Springer; 1999.

[55] McKay MD, Bechman RJ, Conover WJ. A comparison of three methods for selecting values of input variables in the analysis of output from a computer code. Technometrics 1979;21(2):239–45.

[56] Iman RL, Conover WJ. Small sensitivity analysis techniques for computer models with an application to risk assessment. Commun Stat Theor Methods, A 1980;9(17):1749–842.

[57] Tang B. Orthogonal array-based latin hypercubes. J Am Stat Assoc 1993;88(424):1392–7.

[58] Park JS. Optimal latin-hypercube designs for computer experiments. J Stat Plann Inference 1994;39:95–111.

[59] Ye KQ, Li W, Sudjianto A. Algorithmic construction of optimal symmetric latin hypercube designs. J Statist Plann Inferences 2000;90:145–59.

[60] Kalagnanam JR, Diwekar UM. An efficient sampling technique for off-line quality control. Technometrics 1997;39(3):308–19.

[61] Meckesheimer M, Booker AJ, Barton RR, Simpson TW. Computationally inexpensive metamodel assessment strategies. AIAA J 2002;40(10):2053–60.

[62] Fang KT, Lin DKJ, Winker P, Zhang Y. Uniform design: theory and application. Technometrics 2000;39(3):237–48.

[63] Chen VCP, Tsui KL, Barton RR, Meckesheimer M. A review on design, modeling and applications of computer experiments. IIE Trans 2006;38:273–91.

[64] Lin Y. An efficient robust concept exploration method and sequential exploratory experimental design Ph.D. Dissertation Thesis, vol. 780. Atlanta: Mechanical Engineering, Georgia Institute of Technology; 2004.
[65] Jin R, Chen W, Sudjianto A. An efficient algorithm for constructing optimal design of computer experiments. J Statist Plann Inferences 2005;134 (1):268–87.
[66] Sasena M, Parkinson M, Goovaerts P, Papalambros P, Reed M. Adaptive experimental design applied to an ergonomics testing procedure. ASME 2002 Design Engineering Technical Conferences and Computer and Information in Engineering Conference. Montreal, Canada: ASME; 2002. DETC2002/DAC-34091.
[67] Wang GG. Adaptive response surface method using inherited latin hypercube design points. Trans ASME, J Mech Des 2003;125:210–20.
[68] Wang GG, Simpson TW. Fuzzy clustering based hierarchical metamodeling for space reduction and design optimization. J Eng Optim 2004;36(3):313–35.
[69] Jin R, Chen W, Sudjianto A. On sequential sampling for global metamodeling for in engineering design. ASME 2002 Design Engineering Technical Conferences and Computer and Information in Engineering Conference, Montreal, Canada. DETC2002/DAC-34092.
[70] Sacks J, Schiller Susannah B, Welch WJ. Designs for computer experiments. Technometrics 1989;31(1):41–7.
[71] Pronzato L, Müller WG. Design of computer experiments: space filling and beyond. J Stat Comput 2012;22(3):681–701.
[72] Cresssie N. Spatial prediction and ordinary Kriging. Math Geol 1988;20 (4):405–21.
[73] Papadrakakis M, Lagaros M, Tsompanakis Y. Structural optimization using evolution strategies and neural networks. Comput Methods Appl Mech Eng 1998;156(1–4):309–33.
[74] Dyn N, Levin D, Rippa S. Numerical procedures for surface fitting of scattered data by radial basis functions. SIAM J Sci Stat Comput 1986;7(2):639–59.
[75] Fang H, Horstemeyer MF. Global response approximation with radial basis functions. J Eng Optim 2006;38(4):407–24.
[76] Friedman JH. Multivariate adaptive regressive splines. Ann Stat 1991;19 (1):1–67.
[77] De Boor C, Ron A. On multivariate polynomial interpolation. Constr Approximation 1990;6:287–302.
[78] Langley P, Simon HA. Applications of machine learning and rule induction. Commun ACM 1995;38(11):55–64.
[79] Varadarajan S, Chen W, Pelka CJ. Robust concept exploration of propulsion systems with enhanced model approximation capabilities. Eng Optim 2000;32(3):309–34.
[80] Giunta AA, Watson LT. A comparison of approximation modeling techniques: polynomial versus interpolating models. Proceedings of the 7th AIAA/USAF/NASA/ISSMO Symposium on Multidisciplinary Analysis & Optimization, vol. 1. St. Louis, MO: American Institute of Aeronautics and Astronautics Inc; 1998. AIAA-98-4758.
[81] Simpson TW, Mauery TM, Korte JJ, Mistree F. Kriging metamodels for global approximation in simulation-based multidisciplinary design optimization. AIAA J 2001;39(12):2233–41.
[82] Dey S, Mukhopadhyay T, Adhikari S. Stochastic free vibration analyses of composite doubly curved shells – A Kriging model approach. Compos B Eng 2015;70:99–112.
[83] Qian Z, Seepersad CC, Joseph VR, Wu CFJ, Allen JK. Building surrogate models based on detailed and approximate simulations. ASME 2004 Design Engineering Technical Conferences and Computers and Information in Engineering Conference. Salt Lake City, Utah, USA: ASME; 2004. DETC2004-57486.
[84] Martin JD, Simpson TW. Use of Kriging models to approximate deterministic computer models. AIAA J 2005;43(4):853–63.
[85] Li R, Sudjianto A. Penalized likelihood Kriging model for analysis of computer experiments. ASME 2003 Design Engineering Technical Conferences and Computers and Information in Engineering Conference. Chicago, Illinois, USA: ASME; 2003. DETC2003/DAC-48758.
[86] Kleijnen JPC, Van Beers W. Kriging for interpolation in random simulation. J Oper Res Soc 2003;54:255–62.
[87] Daberkow DD, Mavris DN. An Investigation of metamodeling techniques for complex systems design. 9th AIAA/ISSMO Symposium on Multidisciplinary Analysis and Optimization, Atlanta, Georgia, USA. AIAA 2002-5457.
[88] Clarke SM, Griebsch JH, Simpson TW. Analysis of support vector regression for approximation of complex engineering analyses. Trans ASME, J Mech Des 2005;127(6):1077–87.
[89] Pérez VM, Renaud JE, Watson LT. Adaptive experimental design for construction of response surface approximations. AIAA J 2002;40 (12):2495–503.
[90] Mullur AA, Messac A. Extended radial basis functions: more flexible and effective metamodeling. AIAA J 2005;43(6):1306–15.
[91] Turner CJ, Crawford RH. Selecting an appropriate metamodel: the case for NURBS metamodels. ASME 2005 Design Engineering Technical Conferences and Computers and Information in Engineering Conference. Long Beach, California: ASME; 2005. DETC2005-85043.
[92] Morris MD, Mitchell TJ, Ylvisaker D. Bayesian design and analysis of computer experiments: use of derivatives in surface prediction. Technometrics 1993;35 (3):243–55.
[93] Mukhopadhyay T, Dey TK, Chowdhury R, Chakrabarti A, Adhikari S. Optimum design of FRP bridge deck: an efficient RS-HDMR based approach. Struct Multidiscip Optim 2015;52(3):459–77.
[94] Mukhopadhyay T, Chowdhury R, Chakrabarti A. Structural damage identification: a random sampling-high dimensional model representation approach. Adv Struct Eng 2016. http://dx.doi.org/10.1177/1369433216630370.
[95] Wang LP, Grandhi RV, Canfield RA. Multivariate Hermite approximation for design optimization. Int J Numer Methods Eng 1996;39:787–803.
[96] Rasmussen J. Nonlinear programming by cumulative approximation refinement. Struct Optim 1998;15:1–7.
[97] Shin YS, Grandhi RV. A global structural optimization technique using an interval method. Struct Multidiscip Optim 2001;22:351–63.
[98] Huber KP, Berthold MR, Szczerbicka H. Analysis of simulation models with fuzzy graph based metamodeling. Perform Eval 1996;27–28:473–90.
[99] Madu CN. A fuzzy theoretic approach to simulation metamodeling. Appl Math Lett 1995;8(6):35–41.
[100] Kleijnen JPC. Design and analysis of Monte Carlo experiments. In: Gentle JE, Haerdle W, Mori Y, editors. Handbook of Computational Statistics: Concepts and Fundamentals. Heidelberg, Germany: Springer-Verlag; 2004.
[101] Giunta AA, Dudley JM, Narducci R, Grossman B, Haftka RT, Mason WH, Watson LT. Noisy aerodynamic response and smooth approximations in HSCT design. 5th AIAA/USAF/NASA/ISSMO Symposium on Multidisciplinary Analysis and Optimization, vol. 2. Panama City, FL: AIAA; 1994.
[102] Madsen JI, Shyy W, Haftka R. Response surface techniques for diffuser shape optimization. AIAA J 2000;38(9):1512–8.
[103] Jin R, Du X, Chen W. The use of metamodeling techniques for optimization under uncertainty. Struct Multidiscip Optim 2003;25(2):99–116.
[104] Van Beers W, Kleijnen JPC. Kriging interpolation in simulation: a survey. In: Ingalls RG, Rossetti MD, Smith JS, Peters BA, editors. Proceedings of the 2004 Winter Simulation Conference, Washington D. C., USA. p. 113–21.
[105] Dey S, Mukhopadhyay T, Adhikari S. Stochastic free vibration analysis of angle-ply composite plates – A RS-HDMR approach. Compos Struct 2015;122:526–36.
[106] Dey S, Mukhopadhyay T, Khodaparast HH, Adhikari S. Stochastic natural frequency of composite conical shells. Acta Mech 2015;226(8):2537–53.
[107] Dey S, Mukhopadhyay T, Spickenheuer A, Adhikari S, Heinrich G. Bottom up surrogate based approach for stochastic frequency response analysis of laminated composite plates. Compos Struct 2016;140:712–27.
[108] Dey S, Mukhopadhyay T, Khodaparast HH, Kerfriden P, Adhikari S. Rotational and ply-level uncertainty in response of composite shallow conical shells. Compos Struct 2015;131:594–605.
[109] Dey S, Mukhopadhyay T, Sahu SK, Li G, Rabitz H, Adhikari S. Thermal uncertainty quantification in frequency responses of laminated composite plates. Compos B Eng 2015;80:186–97.
[110] Dey S, Mukhopadhyay T, Naskar S, Dey TK, Chalak HD, Adhikari S, Probabilistic characterization for dynamics and stability of laminated soft core sandwich plates, J Sandwich Struct Mater, http://dx.doi.org/10.1177/1099636217694229.
[111] Dey S, Mukhopadhyay T, Sahu SK, Adhikari S. Effect of cutout on stochastic natural frequency of composite curved panels. Compos B Eng 2016;105:188–202.
[112] Dey S, Mukhopadhyay T, Khodaparast HH, Adhikari S. Fuzzy uncertainty propagation in composites using Gram-Schmidt polynomial chaos expansion. Appl Math Model 2016;40(7–8):4412–42.
[113] Dey S, Karmakar A. Natural frequencies of delaminated composite rotating conical shells – A finite element approach. Finite Elem Anal Des 2012;56:41–51.
[114] Meirovitch L. Dynamics and control of structures. NY: John Wiley & Sons; 1992.
[115] Bathe KJ. Finite element procedures in engineering analysis. New Delhi: PHI; 1990.
[116] Giunta AA, Wojtkiewicz SF, Eldred MS, Overview of modern design of experiments methods for computational simulations, American Institute of Aeronautics and Astronautics, Paper AIAA, 2003–0649; 2003.
[117] Santner TJ, Williams B, Notz W. The design and analysis of computer experiments. Heidelberg: Springer; 2003.
[118] Koehler JR, Owen AB. Computer experiments. In: Ghosh S, Rao CR, editors. Handbook of Statistics, vol. 13. Amsterdam: Elsevier Science B.V.; 1996. p. 261–308.
[119] Computational optimization, methods and algorithms, Editors: Slawomir Koziel, Xin-She Yang, ISBN: 978-3-642-20858-4 (Print) 978-3-642-20859-1; 2011.
[120] Jin R, Chen W, Simpson T. Comparative studies of metamodelling techniques under multiple modelling criteria. Struct Multidiscip Optim 2001;23 (1):1–13.
[121] Kim BS, Lee YB, Choi DH. Comparison study on the accuracy of metamodeling technique for non-convex functions. J Mech Sci Technol 2009;23(4):1175–81.
[122] Li Y, Ng S, Xie M, Goh T. A systematic comparison of metamodeling techniques for simulation optimization in decision support systems. Appl Soft Comput 2010;10(4):1257–73.
[123] Li G, Rabitz H. General formulation of HDMR component functions with independent and correlated variables. J Math Chem 2012;50:99–130.
[124] Deutsch F. Best approximation in inner product space. New York: Springer; 2000.
[125] Li G, Wang SW, Rabitz H, Wang S, Jáffe PR. Global uncertainty assessments by high dimensional model representations (HDMR). Chem Eng Sci 2002;57:4445–60.
[126] Wang SW, Levy II H, Li G, Rabitz H. Fully equivalent operational models for atmospheric chemical kinetics within global chemistry-transport models. J Geophys Res 1999;104(D23):30417–26.

[127] Rothman A, Ho TS, Rabitz H. Observable-preserving control of quantum dynamics over a family of related systems. Phys Rev A 2005;72:023416.
[128] Li G, Hu J, Wang SW, Georgopoulos PG, Schoendorf J, Rabitz H. Random sampling-high dimensional model representation (RS-HDMR) and orthogonality of its different order component functions. J Phys Chem A 2006;110:2474–85.
[129] Li G, Artamonov M, Rabitz H, Wang SW, Georgopoulos PG, Demiralp M. High dimensional model representations generated from low order terms – lp-RS-HDMR. J Comput Chem 2003;24:647–56.
[130] Norbert Wiener. The homogeneous chaos. Am J Math 1938;60(4):897–936.
[131] Mahata A, Mukhopadhyay T, Adhikari S. A polynomial chaos expansion based molecular dynamics study for probabilistic strength analysis of nano-twinned copper. Mater Res Express 2016;3:036501.
[132] Matheron GFPM, Traité de géostatistique appliquée, Editions Technip, France, 1962–63. (fundamental tools of linear geostatistics: variography, variances of estimation and dispersion, and kriging).
[133] Cressie NAC. Statistics for spatial data. Revised Edition. New York: Wiley; 1993.
[134] Lichtenstern A. Kriging methods in spatial statistics Bachelor Thesis. Technische Universitat Munchen; 2013.
[135] Friedman JH. Multivariate adaptive regression splines. Ann Stat 1991;19 (1):1–67.
[136] Craven P, Wahba G. Smoothing noisy data with spline functions. Numer Math 1979;31:377–403.
[137] Sudjianto A, Juneja L, Agrawal A, Vora M. Computer aided reliability and robustness assessment. Int J Reliab Quality Saf 1998;5:181–93.
[138] Wang X, Liu Y, Antonsson EK. Fitting functions to data in high dimensional design spaces. Advances in Design Automation (held in Las Vegas, NV). ASME; 1999. Paper No. DETC99/DAC-8622.
[139] Buhmann MD. Radial basis functions. Acta Numerica 2000;1–38.
[140] Hardy RL. Multiquadratic equations of topography and other irregular surfaces. J Geophys 1971;76:1905–15.
[141] Krishnamurthy T. Response surface approximation with augmented and compactly supported radial basis functions. The 44th AIAA/ASME/ASCE/AHS/ASC structures, structural dynamics, and materials conference. Norfolk, VA.
[142] Soo-Chang Kang, Hyun-Moo Koh, Choo Jinkyo F. An efficient response surface method using moving least squares approximation for structural reliability analysis. Probab Eng Mech 2010;25:365–71.
[143] Lancaster P, Salkauskas K. Surfaces generated by moving least squares methods. Math Comput 1981;37(155):141–58.
[144] Breitkpf P, Naceur H, Rassineux A, Villon P. Moving least squares response surface approximation: formulation and metal forming applications. Comput Struct 2005;83:1411–28.
[145] Oh SK, Pedrycz W, Park BJ. Polynomial neural networks architecture, analysis and design. Comput Electr Eng 2003;29(6):703–25.
[146] Manohar B, Divakar S. An artificial neural network analysis of porcine pancreas lipase catalysed esterification of anthranilic acid with methanol. Process Biochem 2005;40(10):3372–6.
[147] Pareek VK, Brungs MP, Adesina AA, Sharma R. Artificial neural network modeling of a multiphase photodegradation System. J Photochem Photobiol A 2002;149:139–46.
[148] Desai KM, Survase SA, Saudagar PS, Lele SS, Singhal RS. Comparison of artificial neural network (ANN) and response surface methodology (RSM) in fermentation media optimization: case study of fermentative production of scleroglucan. Biochem Eng J 2008;41(3):266–73.
[149] Ghaffari A, Abdollahi H, Khoshayand MR, Bozchalooi I Soltani. Performance comparison of neural networks. Environ Sci Technol 2008;42(21):7970–5.
[150] Vapnik VN. Statistical learning theory. Wiley; 1998.
[151] Cherkassky V, Ma Y. Practical selection of SVM parameters and noise estimation for SVM regression. Neural Netw 2004;17:113–26.
[152] Gunn SR. Support vector machines for classification and regression, Technical report, image speech and intelligent systems research group. UK: University of Southampton; 1997.
[153] Qatu MS, Leissa AW. Vibration studies for laminated composite twisted cantilever plates. Int J Mech Sci 1991;33(11):927–40.
[154] Splichal J, Pistek A, Hlinka J. Dynamic tests of composite panels of an aircraft wing. Prog Aerosp Sci 2015;78:50–61.
[155] Daniel IM. Yield and failure criteria for composite materials under static and dynamic loading. Prog Aerosp Sci 2016;81:18–25.
[156] Ochoa OO, Reddy JN. Finite element analysis of composite laminates. Netherlands: Springer; 1992.
[157] Tornabene F, Fantuzzi N, Bacciocchi M, Neves AMA, Ferreira AJM. MLSDQ based on RBFs for the free vibrations of laminated composite doubly-curved shells. Compos B Eng 2016;99:30–47.
[158] Fantuzzi N, Bacciocchi M, Tornabene F, Viola E, Ferreira AJM. Radial basis functions based on differential quadrature method for the free vibration analysis of laminated composite arbitrarily shaped plates. Compos B Eng 2015;78:65–78.
[159] Pandya BN, Kant T. Finite element analysis of laminated composite plates using a higher-order displacement model. Compos Sci Technol 1988;32 (2):137–55.
[160] Kant T, Swaminathan K. Estimation of transverse/interlaminar stresses in laminated composites–a selective review and survey of current developments. Compos Struct 2000;49(1):65–75.
[161] Tornabene F, Fantuzzi N, Viola E, Ferreira AJM. Radial basis function method applied to doubly-curved laminated composite shells and panels with a General Higher-order Equivalent Single Layer formulation. Compos B Eng 2013;55:642–59.
[162] Tornabene F, Liverani A, Caligiana G. FGM and laminated doubly-curved shells and panels of revolution with a free-form meridian: a 2-D GDQ solution for free vibrations. Int J Mech Sci 2011;53(6):446–70.
[163] Tornabene F. Free vibrations of laminated composite doubly-curved shells and panels of revolution via the GDQ Method. Comput Methods Appl Mech Eng 2011;200(9):931–52.
[164] Viola E, Tornabene F, Fantuzzi N. General higher-order shear deformation theories for the free vibration analysis of completely doubly-curved laminated shells and panels. Compos Struct 2013;95(1):639–66.
[165] Tornabene F, Fantuzzi N, Viola E, Reddy JN. Winkler-Pasternak foundation effect on the static and dynamic analyses of laminated doubly-curved and degenerate shells and panels. Compos B Eng 2014;57(1):269–96.
[166] Tornabene F, Fantuzzi N, Bacciocchi M, Viola E. A new approach for treating concentrated loads in doubly-curved composite deep shells with variable radii of curvature. Compos Struct 2015;131(1):433–52.
[167] Dey S, Karmakar A. Free vibration analyses of multiple delaminated angle-ply composite conical shells – A finite element approach. Compos Struct 2012;94 (7):2188–96.
[168] Dey S, Karmakar A. A comparative study on free vibration analysis of delaminated torsion stiff and bending stiff composite shells. J Mech Sci Technol 2013;27(4):963–72.
[169] Dey S, Karmakar A. Finite element analyses of bending stiff composite conical shells with multiple delamination. J Mech Mater Struct 2012;7(2):213–24.
[170] Sriramula S, Chryssanthopoulos KM. Quantification of uncertainty modelling in stochastic analysis of FRP composites. Compos A Appl Sci Manuf 2009;40:1673–84.
[171] Mukhopadhyay T, Naskar S, Dey S, Adhikari S. On quantifying the effect of noise in surrogate based stochastic free vibration analysis of laminated composite shallow shells. Compos Struct 2016;140:798–805.